

Land Misuse and Hydrologic Response: Kaho'olawe, Hawai'i¹

KEITH LOAGUE,² D'ARTAGNAN LLOYD,³ THOMAS W. GIAMBELLUCA,⁴
ANH NGUYEN,⁵ AND BURT SAKATA⁶

DEDICATION: This paper is dedicated to "Ka'imipono" Rendell D. Tong (13 September 1959–4 January 1995). In his lifetime Rendell supported many environmental efforts in Hawai'i, especially the work reported in this paper, with a passion that was contagious. About Kaho'olawe he once wrote: "I'm looking forward to our continued work to restore Hakioawa *ahupua'a* [watershed] and to gain a comprehensive scientific observation and understanding of the hydrologic cycle on Kaho'olawe. We are invigorated and proud to be practicing that foundation of Hawaiian cultural values, *mālama 'āina* [take care of the land]. So we keep working for the land, physically, spiritually . . . for the people of the earth—*e kūpono e ka po'e honua*." The spirit of Ka'imipono lives on in Hawai'i, especially on the island of Kaho'olawe, forever!

ABSTRACT: This paper is concerned with the characterization of near-surface hydrologic response for the Hawaiian island of Kaho'olawe, where erosion caused, in part, by surface runoff is the major factor in landscape denudation. New sets of saturated hydraulic conductivity and sorptivity data from 110 sites across Kaho'olawe are presented and analyzed for spatial structure using statistical methods and land cover classification. At a regional scale there was no statistically characterizable spatial structure in either of the new data sets; we characterized the spatial distribution of saturated hydraulic conductivity and sorptivity based upon land cover. Also presented is a suite of runoff simulations for the entire island of Kaho'olawe, based upon the near-surface soil hydraulic property interpretations reported, for 10 separate rainfall events. The hydrologic response simulator used provides a relatively realistic representation of Hortonian overland flow. This study consisted of 700 deterministic-conceptual rainfall-runoff simulations, based upon the 10 rainfall events applied to 70 catchments that were divided into 1529 overland flow planes. Our simulations suggest, for the large events selected for this study, that the maximum island average surface runoff by the Horton mechanism is ca. 20% of rainfall.

How many years can a mountain exist before it is washed to the sea?

—Bob Dylan

THIS STUDY WAS CONCERNED with identifying runoff-producing areas, via the Horton overland flow mechanism, on the Hawaiian island of Kaho'olawe. In the first part of the paper we describe a field study that was carried out to characterize the near-surface soil hydraulic properties of Kaho'olawe. Measurements of saturated hydraulic conductivity and sorptivity were made at 110 locations on the island and used, with land cover information, to ex-

¹ Manuscript accepted 16 February 1995.

² Department of Geological and Environmental Sciences, Stanford University, Stanford, California.

³ San Francisco, California.

⁴ Department of Geography, University of Hawai'i at Mānoa, Honolulu, Hawai'i.

⁵ Milpitas, California.

⁶ Protect Kaho'olawe 'Ohana, Maui, Hawai'i.

plain the spatial distribution of near-surface soil hydraulic properties. In the second part of the paper we use these near-surface characterizations to excite a quasi-physically based rainfall-runoff model for conceptual simulations of Hortonian overland flow.

The overall strategy of our effort was to conduct a preliminary characterization of near-surface hydrologic processes across Kaho'olawe. This work sets a foundation for an ongoing study concerned with revegetation of the island to arrest devastating erosion problems and a basic investigation of landform development processes for an entire insular system.

Background

Kaho'olawe, the eighth largest island in the Hawaiian chain (see inset in Figure 1), is located ca. 10 km southwest of Cape Kīna'u on the south side of Maui. Erosion caused by surface runoff is a major problem across parts of Kaho'olawe where overgrazing and military activity have caused substantial vegetation loss. It is well understood that overland flow, caused by excess rainfall on exposed soil and subsoil surfaces, leads to sediment transport and reduced likelihood for reestablishing vegetation. Figure 2 illustrates generalized water balance estimates (State of Hawai'i 1990) for Kaho'olawe before and after the devastation of the landscape. Inspection of Figure 2 shows that the lumped pre- and postimpact estimates of runoff are 35 and 75%, respectively. For Kaho'olawe, a quantitative water balance estimate is important for characterizing soil-water recharge and surface runoff. In this study we employed a physically based rainfall-runoff model to focus on the surface water component of the Kaho'olawe water balance. By using a distributed simulation approach coupled to land cover characteristics, we could address the impact of spatially variable near-surface soil hydraulic properties on estimates of surface runoff. Estimates of soil-water recharge and surface runoff are critical to planning revegetation activities and erosion control to accomplish the landscape restoration goals on Kaho'olawe.

A Brief History of Kaho'olawe

Kaho'olawe, 1.5 myr old and 117 km² in area, was first occupied by humans around A.D. 900 (State of Hawai'i 1990). Archaeobotanical evidence suggests that dryland forest gave way to grassland vegetation as a result of agricultural practices of native Hawaiians during the pre-European-contact period (Allen 1987). Spriggs (1987) provided evidence that soil erosion was not a serious problem on the island until traditional Hawaiian land use was replaced by western uses, especially ranching. Abandonment of the traditional Hawaiian land stewardship system in favor of western land tenure in 1848 initiated rapid land-use change on Kaho'olawe. As many as 9,000 goats and 20,000 sheep have inhabited the island at one time (Kaho'olawe Island Conveyance Commission 1993). The resulting soil erosion was severe enough to prompt replanting efforts by the ranchers during the late 1880s. In 1910, the Territorial Board of Agriculture declared that because of overgrazing the island had "become almost worthless through erosion and loss of soil." The island was designated a "Forest Reserve," but failure to control feral goats doomed revegetation efforts. Ranching operations resumed in 1918 and continued until 1941, when the U.S. Navy took possession of the island. Initially used for training of military personnel during World War II, the island continued to be used as a bombing range and small ordnance training site until October 1990. The goat population remained unchecked during most of the navy management period. The damage caused by erosion of land unprotected by vegetation worsened as overgrazing continued. Bombing further degraded vegetation cover and soils.

During the 1970s, Hawaiian protests against military use and mismanagement of Kaho'olawe led to the formation of the Protect Kaho'olawe 'Ohana (PKO). Members of the PKO won a summary judgment in federal court against the navy in 1977 and later negotiated a consent decree as an out-of-court settlement of a civil suit. These actions required the navy to prepare an environmental impact statement to identify and protect his-

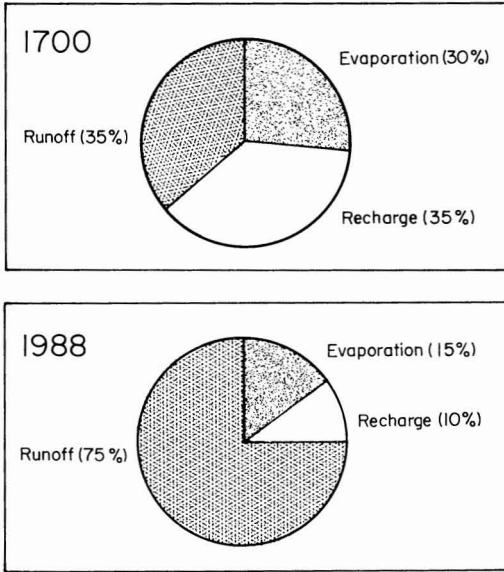


FIGURE 2. Water balance estimates for Kaho'olawe (from State of Hawai'i 1990).

toric and cultural sites, clear ordnance from 41 km² of the island, begin soil conservation and revegetation, eradicate goats, and discontinue ordnance use except in the middle third of the island. In October 1990, by presidential order, bombing and munitions training on the island ceased. Congressional action formed a commission to study issues involved in the conveyance of the island back to Hawai'i.

Anatomy of a PKO Access

The field study reported in this paper was conducted during two trips to Kaho'olawe. Each of these trips is referred to in this paper as an access. The access procedure described here has been used regularly by the PKO during the past 14 yr. Before our field exercises we (K.L., T.W.G., B.S.) visited Kaho'olawe to plan the effort described in this paper. Our first Kaho'olawe access took place 18–20 September 1991; the second access took place 11–14 June 1992. The anatomy of an access is described in the remainder of this section.

The field study team departed for Kaho'olawe at about 0400 hours from two locations

on the island of Maui. The majority of the team left from Mā'alaea (located on the southern coast of West Maui) in the 11-m commercial fishing boat *Pualele*; the crossing took ca. 1 hr. That group brought the study equipment, food, water, and everything else needed for the stay on the island. The remainder of the team left from Mākena (located on the southwestern coast of East Maui) in a PKO zodiac (rubber boat). The zodiac crew arrived at Kaho'olawe first and met the *Pualele* crew ca. 200 m offshore from Hākioawa (located on the northeastern coast of Kaho'olawe), where the team members and equipment were transferred. The zodiac then moved to the reef, where the team entered the surf and swam all the equipment and supplies (in waterproof bags) to shore. Several zodiac trips were required to unload the *Pualele*. On the second access, three trips were required between Mā'alaea and Hākioawa to transport everyone to the island because other activities were scheduled besides the effort reported here. After the unloading was completed, the *Pualele* departed and the zodiac was beached at Hākioawa. At the end of the access, the entire procedure was repeated, in reverse, with the *Pualele* arriving at 0600 hours. During the data collection exercises, the field study team was accompanied by U.S. Navy EOD (Emergency Ordnance Disposal) personnel. Despite the fact that sections of the island have been swept several times (since 1981), ordnance (occasionally undetonated) is still quite prevalent.

STREAMFLOW GENERATION

It is well known (Dunne 1978) that there are three distinct forms by which lateral inflows enter a channel reach in a catchment: (1) groundwater discharge, (2) subsurface stormflow, and (3) overland flow. Groundwater discharge provides the sustaining baseflow component to a stream hydrograph between storm periods. The flashy response of streamflow to individual rainfall events can be ascribed to either subsurface stormflow or overland flow. At most locations, however, the primary source of rapid lateral inflows

is overland flow. Overland flow can only be generated on a hillslope after surface ponding has occurred. It has been recognized for some time (see Freeze 1980) that surface saturation can occur by two quite distinct mechanisms: Horton overland flow and Dunne overland flow. For the Horton mechanism, the rainfall intensity must exceed the saturated conductivity of the surface soil for a period of time long enough for ponding to occur. For the Dunne mechanism, the duration of rainfall, at an intensity less than the saturated hydraulic conductivity, must exceed the period of time necessary for an initially shallow water table to rise to the surface. Horton overland flow is more common on upslope areas within a catchment, generated from areas where surface conductivities are the lowest. Dunne overland flow is more common in near-channel lowlands, generated from areas where the water table is the shallowest. Both the Horton and Dunne mechanisms can lead to variable source areas that expand and contract through wet and dry periods.

It is our belief that the primary form of streamflow generation on Kaho'olawe, where erosion is important, is overland flow. We feel that the Horton mechanism is the dominant overland flow process for many areas across Kaho'olawe because of low surface conductivities and a deep water table.

Rainfall-Runoff Model: Hortonian Overland Flow

The conceptual structure of the quasi-physically based rainfall-runoff model (QPBRM) used in this study is similar to that described by Engman (1974). K.L. employed an earlier version of QPBRM extensively for a small rangeland catchment (R-5) in Oklahoma (Loague and Freeze 1985, Loague 1990, 1992a,b,c). In the study reported here we used QPBRM to investigate how much Horton runoff is likely to occur on Kaho'olawe. The operating algorithms for QPBRM are based on solutions and/or simplifications to the full set of coupled partial differential equations that describe near-surface hydrologic response. The model has three major components: (1) an infiltration algorithm that

allows calculation of the rainfall excess by difference, (2) a routing algorithm that translates partial area rainfall excess, generated on the overland flow planes, into lateral inflow hydrographs at the stream channel, and (3) a routing algorithm for tracking the streamflow hydrograph through the channel system.

The three major components of QPBRM each rest upon one-dimensional equations that, when coupled together, result in a quasi-three-dimensional representation of rainfall runoff via the Horton mechanism. The infiltration equation is similar to Philip's two-parameter equation, which is a particular solution to Richards' equation for vertical flow in an unsaturated-saturated soil profile. The equations for overland and channel flow routing are each based upon numerical solution to kinematic forms of the shallow water equations. The model allows partial source areas to expand and contract during a storm. Implementation of QPBRM for a given Kaho'olawe catchment is accomplished using a set of overland flow planes that divide the areas of interest into segments. The simulation philosophy of QPBRM as used in this effort is that of a conceptually sound model that does not depend upon the calibration of catchment parameters with historical rainfall-runoff records. The underlying and operating equations that compose QPBRM are presented in the following two subsections.

UNSATURATED SOIL-WATER FLOW. Richards' equation for one-dimensional vertical unsaturated soil-water flow, based upon combining the transient continuity equation for fluid flow in porous media with the unsaturated version of Darcy's law, is:

$$\frac{\partial}{\partial z} \left[K(F_i, \psi) \left\{ \frac{\partial \psi}{\partial z} + 1 \right\} \right] = C(F_i, \psi) \frac{\partial \psi}{\partial t} \quad (1)$$

where z [L] is the vertical distance from the soil surface downward, ψ [L] is pressure head, $K(\psi)$ [LT^{-1}] and $C(\psi)$ [L^{-1}] are functional relationships for hydraulic conductivity and specific soil-water content, respectively, and F_i represents the different homogeneous formations that make up a heterogeneous system. The hydraulic head (h), the potential relationship that governs fluid flow in porous

media, is related to the pressure head as follows: $h = \psi + z$, where z is the elevation head measured from a reference datum to the point of measurement.

The infiltration algorithm used in QPBRRM, similar to Philip's two-parameter equation, is:

$$i = 0.5 S t^{-1/2} + 0.5 K_s \quad (2)$$

where i [LT^{-1}] is the infiltration rate, S [$LT^{-1/2}$] is the sorptivity, and K_s [LT^{-1}] is taken here as the saturated hydraulic conductivity. Equation 2 is an analytical solution to equation 1, written in terms of soil-water content instead of pressure head, for uniform nonswelling soil profiles with infiltration events that produce incipient surface ponding.

OPEN CHANNEL AND OVERLAND FLOW. Flow of water over a surface or in a channel is described by two partial differential equations (continuity and momentum) based upon the following four assumptions: (1) the velocity at any section is uniform and unidirectional, (2) the channel slope is small, (3) stream line curvatures are small, and (4) energy losses are represented by the slope of the energy gradient times the length of the channel reach.

The continuity equation is:

$$A \frac{\partial V}{\partial x} + V \frac{\partial A}{\partial x} + A \frac{\partial A}{\partial t} = q \quad (3)$$

where A [L^2] is the cross-sectional flow area, V [LT^{-1}] is the average velocity, x [L] is the horizontal distance along the channel, and q [L^3T^{-1}] is the source term.

The momentum equation is:

$$\frac{1}{g} \frac{\partial V}{\partial t} + V \frac{\partial V}{\partial x} + \frac{g}{A} \frac{\partial}{\partial x} (A \bar{y}) + \frac{Vq}{A} = S_o - S_f \quad (4)$$

where g [LT^{-2}] is the acceleration due to gravity, \bar{y} [L] is the depth of water to the centroid of the volume, S_o [dimensionless] is the bed slope of the channel, and S_f [dimensionless] is the friction slope. Equations 3 and 4 are known collectively as the Saint Venant or shallow water equations. Mathematically the shallow water equations describe the propagation of a wave; they cannot be solved in closed form for practical sit-

uations. Kinematic approximations are often used to represent the shallow water equations for overland and channel flow. The kinematic equations take the form of first-order differential equations, computationally much simpler than the complete hyperbolic shallow water equations. Kinematic flow occurs whenever a balance is achieved between gravitational and frictional forces.

In their kinematic forms, the equations of continuity and motion used in QPBRRM for overland flow are given, respectively, as:

$$Q = Q_n \quad (5)$$

$$\frac{\partial Q}{\partial x} + \frac{\partial y}{\partial t} = q \quad (6)$$

where Q [L^3T^{-1}] is discharge, Q_n [L^3T^{-1}] is normal discharge, y [L] is the depth of water, and q is the source term. The source term in a QPBRRM simulation is the precipitation excess calculated by difference from equation 2. Turbulent flow is assumed; therefore equation 5 is written in the form:

$$Q = \frac{1}{n_o} y^{1.67} S_o^{1/2} \quad (7)$$

where n_o [dimensionless] is the Manning's roughness coefficient for the overland flow planes.

In their kinematic forms the equations of continuity and motion used in QPBRRM for open channel flow are given, respectively, as:

$$Q = Q(A) \quad (8)$$

$$\frac{\partial Q}{\partial x} + \frac{\partial A}{\partial t} = q \quad (9)$$

The source term used in QPBRRM is now the lateral inflow to the channel from the overland flow equations and precipitation falling directly on the channel. Turbulent flow is assumed; therefore equation 8 is written as:

$$Q = \frac{1}{n_c} R^{0.67} S_o^{1/2} \quad (10)$$

where R [L] is the hydraulic radius of the channel and n_c is the Manning's roughness coefficient for the channel sections.

The overland flow and open channel flow algorithms for QPBRRM are based upon

explicit finite-difference numerical approximations to equations 6 and 7 and 9 and 10, respectively. To achieve stability with the explicit schemes, the following criterion (Engman 1974) was employed:

$$10 \leq \frac{\Delta t}{\Delta x \cdot n} \leq 25 \quad (11)$$

where Δt is the time step, Δx is the space increment, and n is the Manning's roughness coefficient ($n = n_c$ for channel; $n = n_o$ for overland).

KAHO'OLAWA: CHARACTERISTICS AND FIELD STUDY

Geology and Hydrology

The geology and hydrology for the state of Hawai'i have been described by Stearns (1985), Macdonald et al. (1983), and Armstrong (1983). The geology and groundwater resources for the Hawaiian island of Kaho'olawe were described by Stearns (1940). Kaho'olawe is 18 km long and 10 km wide with a maximum elevation of 454 m and a semiarid climate. Marine erosion has cut cliffs as high as 240 m along the eastern and southern shores. Kaho'olawe is a shield-shaped extinct volcano composed chiefly of thin flows of primitive basalt poured in rapid succession from three rift zones and a vent at their intersection. The entire summit of the island has been eroded to a hardpan surface. A geologic map of Kaho'olawe is shown in Figure 1. The slopes of Kaho'olawe are corrugated with gulches 15 to 60 m deep cut by ephemeral streams whose drainage pattern radiates from Lua Makika (Figure 1). The average annual rainfall for Kaho'olawe is estimated to be ca. 750 mm/yr. Constant strong winds have caused widespread soil erosion following the loss of vegetation caused by overgrazing. Resistivity surveys and wells have indicated that groundwater is mostly brackish (Kauahikaua 1989).

Land Cover

Figure 3 shows the island-wide land cover distribution map constructed for this study.

The 18 land cover classifications shown in Figure 3 and listed in Table 1 were selected based upon observations made during numerous site visits. Land classes were identified and mapped at regional scale on the basis of the color and textural appearance of land cover, using a 1986 set of low-altitude color air photos made by the U.S. Navy. Stereo pairs were viewed to verify our interpretations. A vertical sketchmaster was used to transfer the air photo details to the planimetric map. The base map was the 1984 U.S. Geological Survey 1:25,000 metric topographic map for Kaho'olawe. Arc/Info software was used in our land cover mapping; the areas of different land cover were achieved through the Calculate function of the Arc/Info package. The details of the criteria used in our land cover classification are given in the footnote in Table 1. In this study we used land cover as a surrogate for near-surface soil hydraulic property distributions in space; relationships between sparse (yet precious) soil hydraulic property measurements and land cover were established and extrapolated.

Field Measurements

DISK PERMEAMETER. Saturated hydraulic conductivity and sorptivity were measured at 110 sites across Kaho'olawe using four CSIRO disk permeameters. The saturated hydraulic conductivity (K_s) estimates are based upon the following relationship:

$$K_s = \frac{q}{\pi r^2} - \frac{4bS^2}{\pi r(\theta_n - \theta_i)} \quad (12)$$

where q is the flow rate [L^3/T], π is 3.14, r is the radius of the permeameter ring [L], b is a constant (0.55), S is sorptivity [$L/T^{1/2}$], θ_i is the volumetric soil-water content at the start of the measurement [dimensionless], and θ_n is the volumetric soil-water content at the end of the measurement [dimensionless]. The radius of the permeameter ring in this study was 0.1 m. The sorptivity is calculated from the early time data by plotting $Q/\pi r^2$ versus the square root of time, where Q [L^3] is the cumulative volume of water used in the measurement. The theory and design of the CSIRO disk permeameter was discussed by Perroux

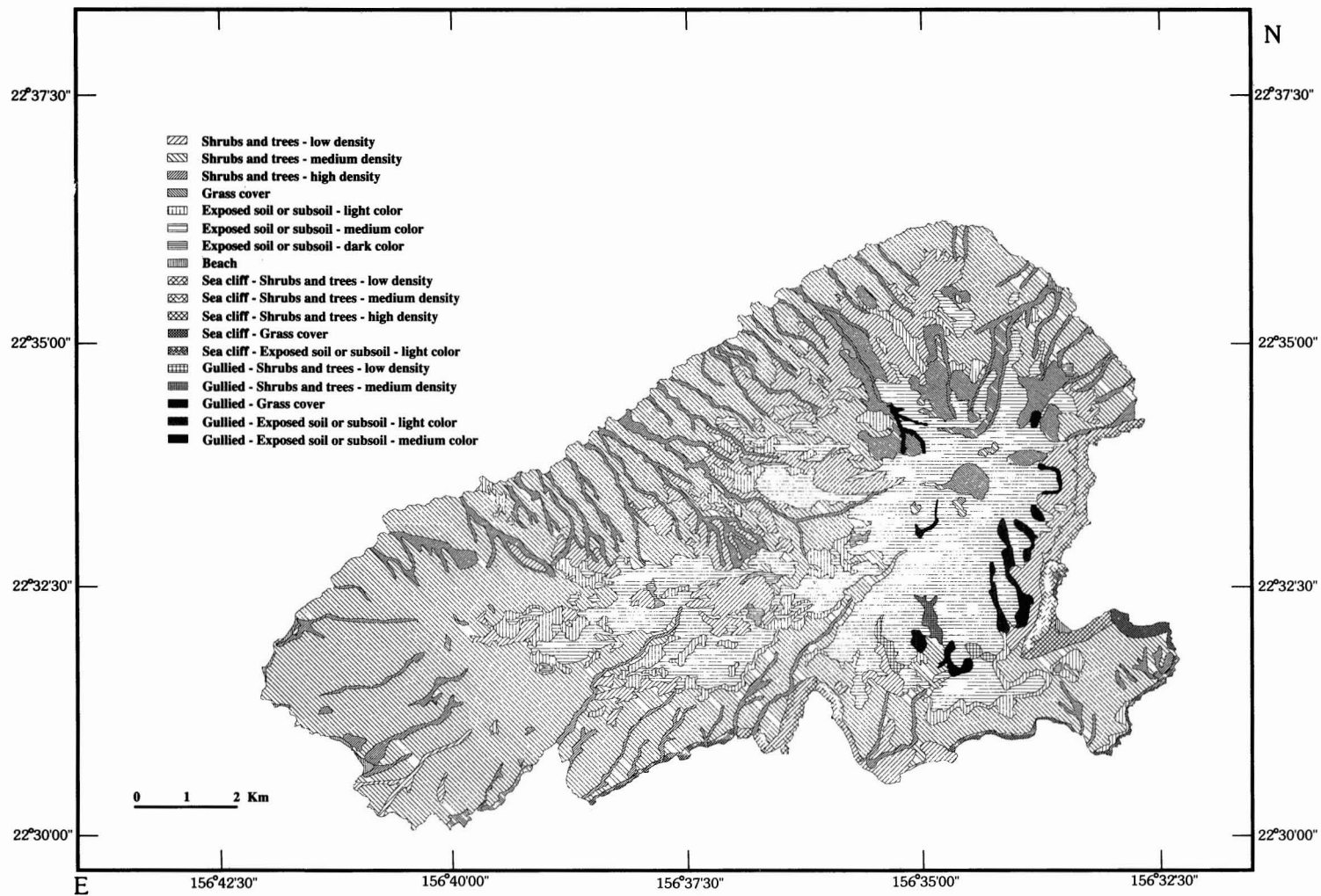


FIGURE 3. Land cover classification for Kaho'olawe based upon air photo interpretation.

TABLE 1

LAND COVER CLASSIFICATIONS FOR KAHŌ'OLAWĒ AS SHOWN ON FIGURE 3, BASED UPON AIR PHOTO INTERPRETATION

LAND COVER CLASS	DESCRIPTION	PERCENTAGE OF ISLAND
1	Exposed soil or subsoil, dark color	0.5
2	Exposed soil or subsoil, medium color	19.9
3	Gullied—exposed soil or subsoil, medium color	0.1
4	Exposed soil or subsoil, light color	4.6
5	Gullied—exposed soil or subsoil, light color	0.8
6	Sea cliff—exposed soil or subsoil, light color	0.6
7	Shrubs and trees, high density	8.0
8	Sea cliff—shrubs and trees, high density	0.4
9	Shrubs and trees, medium density	46.6
10	Gullied—shrubs and trees, medium density	0.2
11	Sea cliff—shrubs and trees, medium density	0.7
12	Shrubs and trees, low density	11.6
13	Gullied—shrubs and trees, low density	0.2
14	Sea cliff—shrubs and trees, low density	1.3
15	Grass	3.8
16	Gullied—grass	0.2
17	Sea cliff—grass	0.3
18	Beach	0.2

Exposed soil or subsoil, easily identified on the basis of color; further subdivision made on the basis of color: dark, dark brown; medium, yellowish brown; light, yellow. Shrubs and trees, identified on the basis of dark green color and coarse texture: high, complete vegetation coverage, no exposed soil; medium, vegetation coverage between 70 and 100%; low, vegetation coverage between 50 and 70%. Grass, identified on the basis of light color and fine texture; verified with stereoscopic examination. Beach, identified on the basis of proximity to coast, tan color, and very fine texture. Gullied, gullies are easily identifiable in air photos. Sea cliff, identified on the basis of proximity to the coast and on slope.

and White (1988) and White et al. (1992). The major advantages of the disk permeameter in this study were that little water is needed to complete a measurement and only minor surface disturbance is required; a disadvantage was the small size of the measurement area.

TIME DOMAIN REFLECTOMETRY. Volumetric soil-water content was measured at the start (θ_i) and end (θ_n) of each disk permeameter measurement using the Trase System 1 (Soil-moisture 1990, Skaling 1992). The Trase System 1 is a time domain reflectometry (TDR) approach to making indirect soil-water content measurements. TDR is an in situ technique for measuring near-surface soil-water contents via the electromagnetic properties of the soil. The reader interested in a detailed review of TDR is directed to Dalton (1992) and Zegelin et al. (1992).

One might question the use of an electromagnetic technique in soils known to be high in iron, such as those found in Hawai'i.

However, studies in Hawai'i (R. E. Green, pers. comm., 1992) have suggested that the TDR method can provide good estimates of soil-water content for soils high in iron. For some measurements in this study, the θ_n estimates are low because the depth of the TDR wave guides (0.15 m) was deeper than the position of the wetting front at the end of the disk permeameter measurement. With θ_n underestimated, the K_s values, estimated from equation 12, are underestimated.

Results

The saturated hydraulic conductivity and sorptivity values determined for the 110 Kaho'olawe measurement sites (Figure 4) are given in Table 2. The general selection of measurement sites was based upon our desire to represent the spatial variations in land cover, taken loosely as a surrogate for saturated hydraulic conductivity, and strict time constraints.

Inspection of Table 2 shows that there

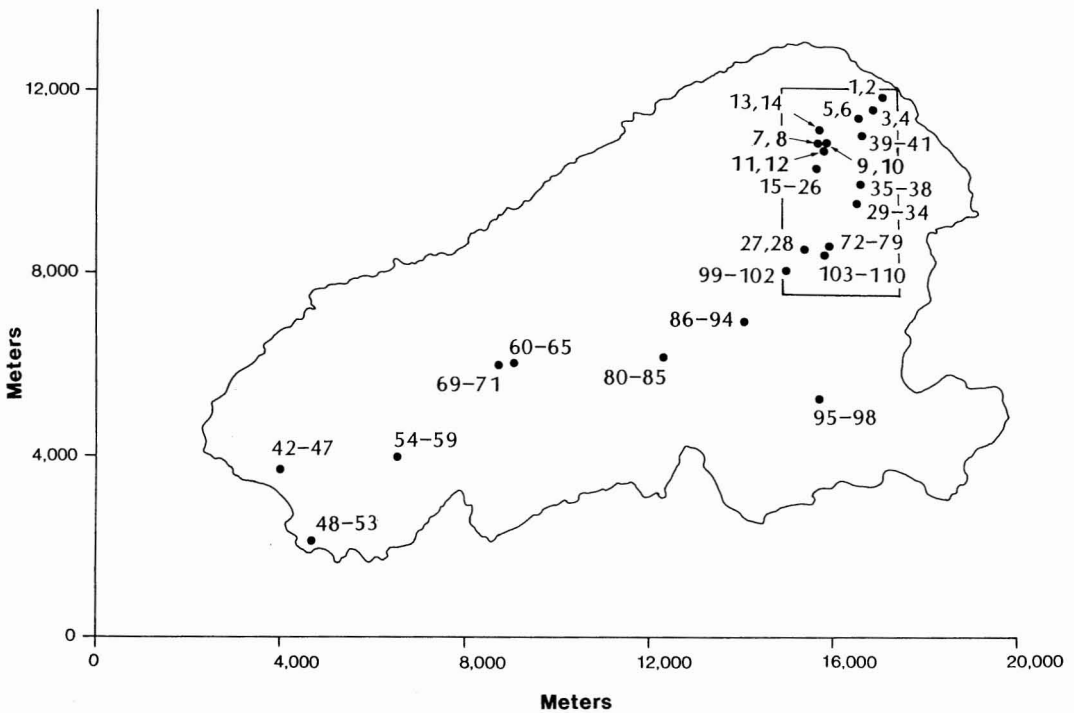


FIGURE 4. Locations of saturated hydraulic conductivity and sorptivity measurements and the intensive study area (box).

is tremendous variability in the saturated hydraulic conductivity measurements across Kaho'olawe; the maximum and minimum values are 4.1×10^{-3} and 1.2×10^{-8} m sec^{-1} , respectively. The mean (arithmetic) saturated hydraulic conductivity value for the 110 estimates is 8.0×10^{-5} m sec^{-1} ; the uncertainty in these estimates (represented by the standard deviation) is 4.1×10^{-4} m sec^{-1} . The coefficient of variation (standard deviation/mean) for the saturated hydraulic conductivity data is 5.1. The sorptivity estimates in Table 2 show some variability; the maximum and minimum values are 6.2×10^{-3} and 1.1×10^{-4} $\text{m sec}^{-1/2}$, respectively. The mean sorptivity value for the 110 estimates is 1.4×10^{-3} $\text{m sec}^{-1/2}$; the standard deviation is 8.6×10^{-4} $\text{m sec}^{-1/2}$. The coefficient of variation for the sorptivity data is 0.5. The mean values for the saturated hydraulic conductivity and sorptivity data reported here compare very well (R. E. Green, pers. comm., 1993)

with similar measurements made in Hawai'i on other islands for similar soils (for example, see Green et al. 1982).

An intensive study area (13.8 km^2) for Kaho'olawe, generally coincident with the Hakioawa catchment (no. 4 on Figure 8), containing 61 of the 110 measurement sites is outlined in Figure 4. The statistical characteristics for the saturated hydraulic conductivity and sorptivity data from the intensive study area are given in Table 3. The summary statistics in Table 3 are generally quite similar to those in Table 2.

Of the 18 land covers listed in Table 1, only five (nos. 2, 4, 9, 12, and 15) are represented by the 110 measurements made during our two accesses. It was not possible to establish multiple measurement sites for all the land-cover classifications listed in Table 1 because of the time limitations of the two Kaho'olawe accesses. Therefore, we grouped the 18 classifications in Table 1 into the three

TABLE 2

SATURATED HYDRAULIC CONDUCTIVITY AND SORPTIVITY ESTIMATES FROM TWO KAHOLAWE ACCESSES

MEASUREMENT ^a NO.	LOCATION ^b (m; x, y)	SATURATED HYDRAULIC CONDUCTIVITY, K_s (m sec ⁻¹)	SORPTIVITY, S (m sec ^{-1/2})	LAND COVER CLASSIFICATION ^c
1	17200, 11975	2.3E-5 ^d	1.3E-3	C
2	17210, 11975	1.3E-6	1.6E-3	C
3	17000, 11700	4.6E-6	9.2E-4	A
4	17010, 11700	1.3E-5	1.6E-3	A
5	16675, 11475	2.1E-5	1.4E-3	A
6	16685, 11475	8.9E-7	7.5E-4	A
7	15875, 10925	1.6E-5	8.2E-4	B
8	15885, 10925	2.6E-6	7.0E-4	B
9	15950, 10925	1.8E-5	1.3E-3	A
10	15960, 10925	2.2E-6	5.6E-4	A
11	15900, 10900	1.6E-6	1.8E-3	C
12	15910, 10900	6.3E-5	1.9E-3	C
13	15825, 11150	1.7E-7	7.0E-4	A
14	15835, 11150	2.0E-5	8.9E-4	A
15	15775, 10375	1.3E-5	1.1E-3	C
16	15785, 10375	5.0E-6	1.4E-3	C
17	15765, 10375	2.7E-6	1.4E-3	C
18	15775, 10365	2.2E-5	2.3E-3	C
19	15775, 10385	1.1E-5	2.0E-3	C
20	15765, 10385	5.6E-4	3.1E-3	C
21	15785, 10385	3.3E-5	1.6E-3	C
22	15765, 10365	2.7E-5	1.3E-3	C
23	15785, 10365	3.2E-7	1.7E-3	C
24	15765, 10395	1.7E-5	1.4E-3	C
25	15775, 10395	2.6E-5	1.3E-3	C
26	15785, 10395	2.6E-5	1.3E-3	C
27	15525, 8600	2.4E-5	1.1E-4	A
28	15535, 8600	1.7E-6	1.9E-4	A
29	16585, 9595	3.3E-5	1.9E-3	C
30	16600, 9600	8.7E-5	4.4E-3	C
31	16615, 9610	1.9E-6	2.6E-4	A
32	16620, 9620	3.0E-6	3.3E-4	A
33	16595, 9595	8.9E-6	1.6E-3	C
34	16610, 9600	7.8E-5	1.7E-3	C
35	16695, 10025	1.2E-5	7.8E-4	A
36	16700, 10025	9.9E-6	7.1E-4	A
37	16700, 10030	9.4E-6	1.5E-3	B
38	16705, 10025	1.5E-5	9.5E-4	A
39	16635, 11095	3.1E-5	1.3E-3	A
40	16645, 11080	1.5E-5	7.5E-4	A
41	16640, 11075	2.5E-5	1.9E-3	A
42	4055, 4750	7.3E-5	6.2E-3	C
43	4050, 4735	9.1E-4	3.8E-4	B
44	4055, 4735	4.1E-5	2.8E-3	B
45	4065, 4750	2.2E-4	2.8E-3	C
46	4060, 4735	1.8E-4	3.4E-3	B
47	4065, 4735	6.0E-4	3.3E-3	B
48	4685, 2155	3.6E-5	1.3E-3	B
49	4685, 2140	1.1E-6	7.1E-4	B
50	4705, 2175	3.7E-7	8.7E-4	C
51	4680, 2155	1.6E-5	1.4E-3	B
52	4705, 2170	3.9E-5	1.4E-3	B
53	4715, 2170	3.9E-6	6.6E-4	A
54	6625, 3965	3.6E-6	9.1E-4	B
55	6595, 3970	1.0E-5	1.4E-3	A

TABLE 2 (continued)

MEASUREMENT ^d NO.	LOCATION ^b (m; x, y)	SATURATED HYDRAULIC CONDUCTIVITY, K_s (m sec ⁻¹)	SORPTIVITY, S (m sec ^{-1/2})	LAND COVER CLASSIFICATION ^c
56	6590, 3985	1.2E-5	1.3E-3	C
57	6615, 3960	1.2E-5	1.4E-3	B
58	6585, 3975	1.4E-5	1.2E-3	B
59	6595, 3975	1.5E-5	3.8E-4	C
60	9135, 6035	3.0E-5	1.8E-3	B
61	9135, 6030	2.6E-5	6.9E-4	A
62	9145, 6035	1.1E-5	7.3E-4	A
63	9140, 6035	3.6E-5	1.9E-3	B
64	9140, 6030	2.7E-5	1.0E-3	A
65	9145, 6040	2.6E-7	1.2E-3	A
66	8920, 5975	2.4E-6	1.2E-3	A
67	8905, 5940	5.0E-6	8.2E-4	A
68	8925, 5955	2.6E-5	1.7E-3	A
69	8920, 5980	1.1E-5	6.3E-4	A
70	8905, 5935	7.4E-5	2.3E-3	C
71	8925, 5960	3.4E-5	1.4E-3	A
72	15980, 8640	5.1E-5	2.0E-3	A
73	15995, 8640	1.2E-6	8.9E-4	A
74	16020, 8640	1.3E-6	5.8E-4	A
75	16035, 8640	8.6E-6	1.4E-3	A
76	15965, 8640	3.1E-5	9.1E-4	A
77	15950, 8640	9.2E-7	4.2E-4	A
78	16015, 8640	4.1E-3	8.0E-4	A
79	16040, 8640	9.3E-8	5.7E-4	A
80	12415, 6205	7.9E-6	5.7E-4	A
81	12420, 6205	2.8E-6	3.7E-4	A
82	12415, 6200	7.1E-5	1.6E-3	A
83	12420, 6195	2.7E-5	1.6E-3	A
84	12425, 6205	4.2E-5	1.5E-3	A
85	12420, 6200	5.6E-7	1.4E-3	C
86	14110, 6920	2.1E-5	1.5E-3	A
87	14140, 6940	1.1E-6	1.5E-3	A
88	14125, 6930	1.8E-5	1.2E-3	A
89	14150, 6950	1.7E-5	1.2E-3	C
90	14120, 6920	3.0E-5	2.4E-3	A
91	14150, 6940	4.2E-6	1.4E-3	C
92	14135, 6930	2.2E-6	7.4E-4	A
93	14160, 6950	1.4E-6	9.7E-4	C
94	14115, 6930	1.2E-8	5.9E-4	A
95	15755, 5300	3.8E-5	2.5E-4	C
96	15750, 5310	2.3E-5	1.7E-3	C
97	15750, 5315	1.2E-6	1.0E-3	C
98	15765, 5320	4.0E-5	2.0E-3	C
99	15135, 8110	6.0E-5	1.0E-3	C
100	16120, 8100	4.1E-5	1.0E-3	C
101	15125, 8110	2.4E-5	6.1E-4	A
102	15135, 8130	6.3E-7	2.2E-3	C
103	15935, 8510	1.1E-5	1.6E-3	A
104	15965, 8515	1.0E-5	2.3E-3	C
105	15945, 8510	6.8E-6	1.7E-3	B
106	15955, 8510	2.6E-5	2.3E-3	C
107	15940, 8510	1.1E-5	2.3E-3	C
108	15970, 8515	1.7E-4	2.0E-3	B
109	15950, 8510	5.8E-6	2.3E-3	C
110	15960, 8510	3.8E-5	1.6E-3	C

TABLE 2 (continued)

MEASUREMENT ^a NO.	LOCATION ^b (m; x, y)	SATURATED HYDRAULIC CONDUCTIVITY, K_s (m sec ⁻¹)	SORPTIVITY, S (m sec ^{-1/2})	LAND COVER CLASSIFICATION ^c
Arithmetic mean		8.0E-5	1.4E-3	
Harmonic mean		8.5E-7	9.1E-4	
Geometric mean		1.1E-5	1.2E-3	
Standard deviation		4.1E-4	8.6E-4	
Maximum value		4.1E-3	6.2E-3	
Minimum value		1.2E-8	1.1E-4	
Median		1.5E-5	1.3E-3	
Coefficient of variation ^a		5.1	0.5	

^aMeasurements 1–28, 18–20 September 1991; measurements 29–110, 11–14 June 1992. ^bSee Figure 4.

^cSee Table 4. ^d2.3E-5 = 2.3×10^{-5} . ^eStandard deviation/arithmetic mean (dimensionless).

TABLE 3

SUMMARY STATISTICS FOR THE 61 SATURATED HYDRAULIC CONDUCTIVITY AND SORPTIVITY ESTIMATES FROM THE INTENSIVE STUDY AREA IDENTIFIED IN FIGURE 4

STATISTIC	SATURATED HYDRAULIC CONDUCTIVITY, K_s (m sec ⁻¹)	SORPTIVITY, S (m sec ^{-1/2})
Arithmetic mean	9.7E-5 ^a	1.4E-3
Harmonic mean	1.9E-6	8.6E-4
Geometric mean	1.1E-5	1.1E-3
Standard deviation	5.3E-4	7.5E-4
Maximum value	4.1E-3	4.4E-3
Minimum value	9.3E-8	1.1E-4
Median	1.3E-5	1.3E-3
Coefficient of variation ^b	5.5	0.5

^a9.7E-5 = 9.7×10^{-5} .

^bStandard deviation/arithmetic mean (dimensionless).

revised land-cover classifications listed in Table 4. Our criteria for these groupings are summarized in the footnote to Table 4. The land-cover classifications in Table 4 are used to group the estimates of saturated hydraulic conductivity and sorptivity into three classes.

The spatial structure of saturated hydraulic conductivity and sorptivity across the entire island of Kaho'olawe and the intensive study area are represented by the two-dimensional directional semivariograms shown in Figures 5 and 6. The statistical characteristics of the 110 saturated hydraulic conductivity and sorptivity estimates, based upon the land-cover classifications in Table 4, are given in Table 5.

The data in Table 5 and Figures 5 and 6 lead to the following generalized comments: (1) There appears to be little spatial structure,

TABLE 4

LAND COVER CLASSIFICATION (BASED UPON FIELD OBSERVATION AND HYDRAULIC SIGNIFICANCE) USED TO GROUP SATURATED HYDRAULIC CONDUCTIVITY AND SORPTIVITY ESTIMATES

LAND COVER	DESCRIPTION	PERCENTAGE OF ISLAND	USED TO REPRESENT CLASSIFICATIONS IN TABLE 1
A	Exposed soil or subsoil	26.5	1–16
B	Shrubs and trees	69.0	7–14
C	Grass	4.5	15–18

Exposed soil or subsoil: hard, relatively impervious clay or saprolite, with little or no vegetative cover (surface usually marked with intersecting cracks with ca. 1-m spacing, occurs in broad, gently sloping surfaces in higher elevations and in steep, deeply gullied middle elevations). Shrubs and trees: ca. 2- to 4-m-high woody vegetation of various coverages, often with grass understory (usually associated with soil remnant having B [or even A] horizon still intact). Grass: ca. 1- to 2-m-high grass (often associated with soil having B horizon still intact).

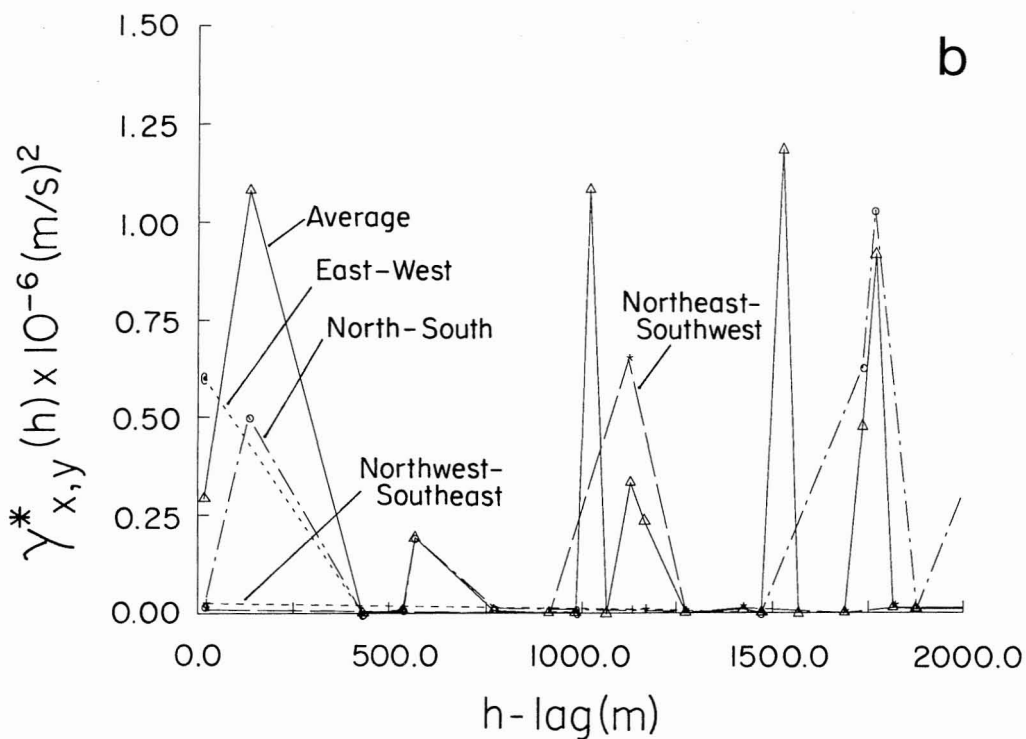
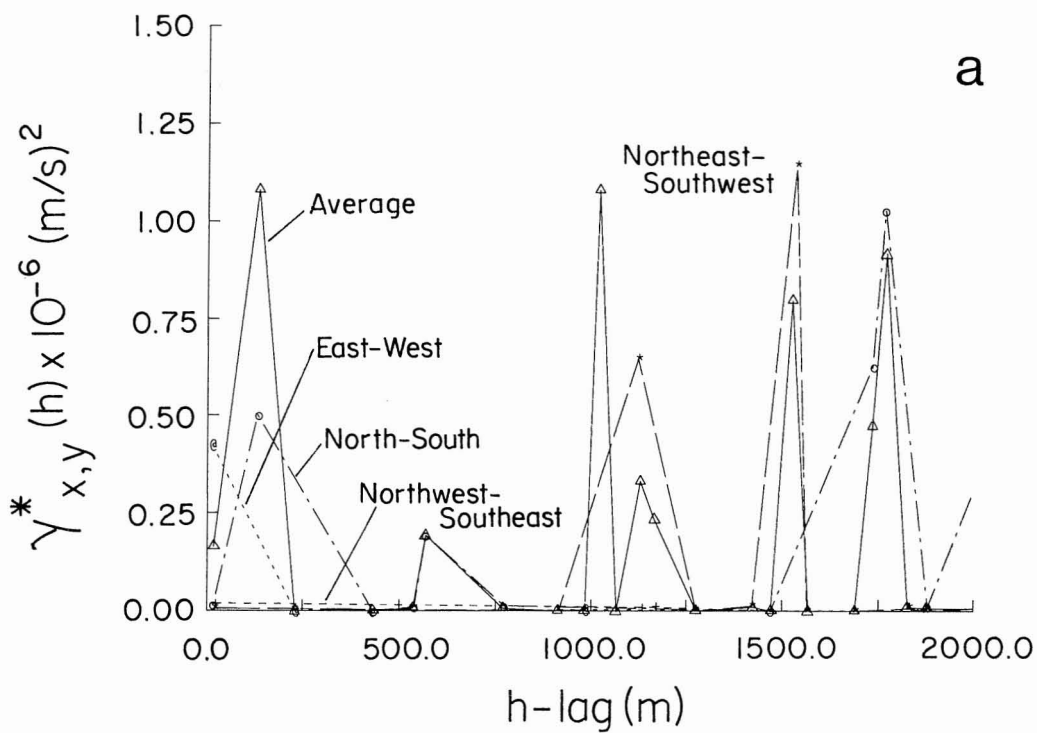


FIGURE 5. Directional semivariograms for saturated hydraulic conductivity estimates: (a) island, 110 measurement sites; (b) intensive study area, 61 measurement sites.

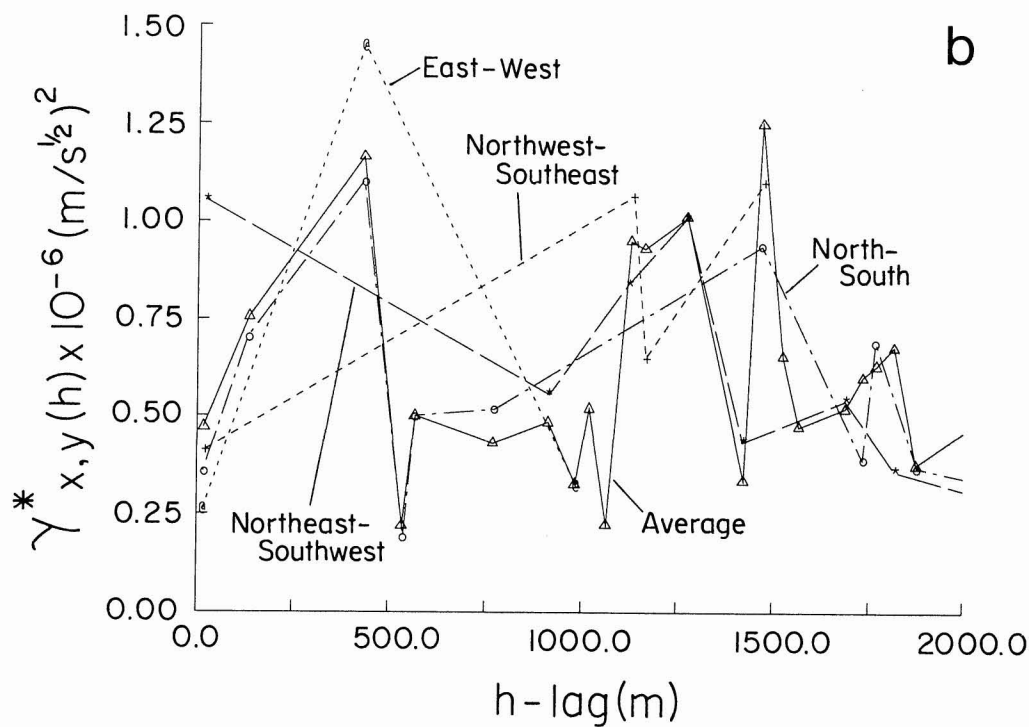
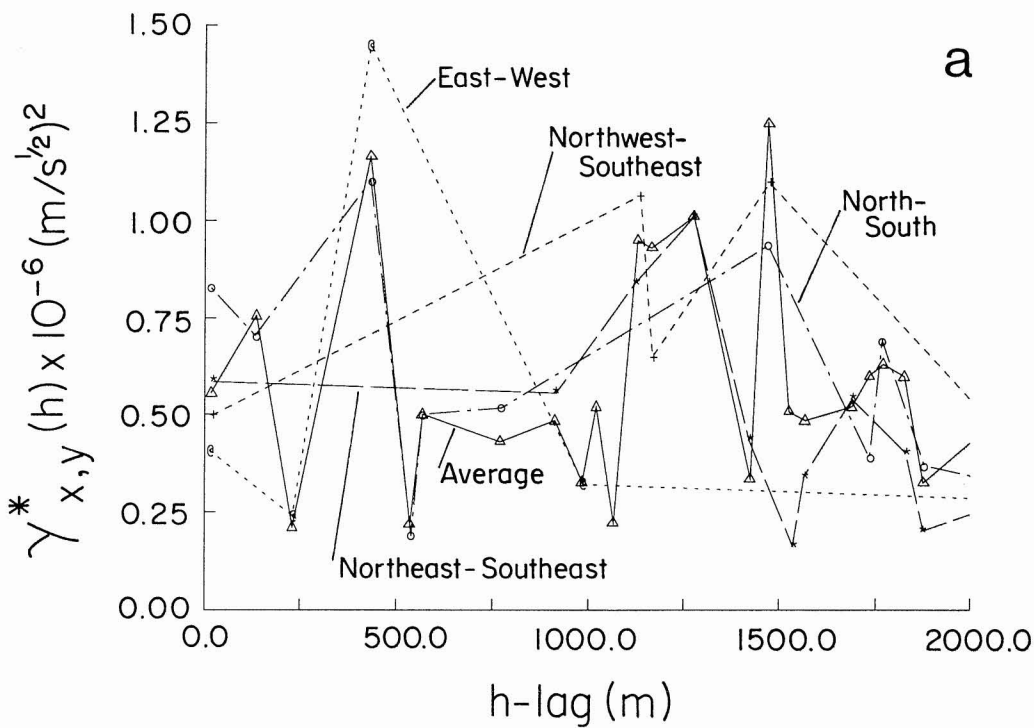


FIGURE 6. Directional semivariograms for sorptivity estimates: (a) island, 110 measurement sites; (b) intensive study area, 61 measurement sites.

TABLE 5

STATISTICAL CHARACTERISTICS OF SATURATED HYDRAULIC CONDUCTIVITY AND SORPTIVITY ESTIMATES BASED UPON LAND COVER

LAND COVER ^a	SATURATED HYDRAULIC CONDUCTIVITY (K_s)					SORPTIVITY (S)				
	NO. OF MEASUREMENTS	MEAN VALUES (m sec ⁻¹)	STANDARD DEVIATION (m sec ⁻¹)	COEFFICIENT OF VARIATION (DIMENSIONLESS)	MAXIMUM AND MINIMUM VALUES (m sec ⁻¹)	NO. OF MEASUREMENTS	MEAN VALUES (m sec ^{-1/2})	STANDARD DEVIATION (m sec ^{-1/2})	COEFFICIENT OF VARIATION (DIMENSIONLESS)	MAXIMUM AND MINIMUM VALUES (m sec ^{-1/2})
A	51	9.6E-5 ^b	5.8E-4	6.0	4.1E-3	51	1.0E-3 ^b	5.0E-4	0.5	2.4E-3
		4.5E-7 ^c			1.2E-8		6.9E-4 ^c			1.1E-4
		7.4E-6 ^d					8.6E-4 ^d			
		1.1E-5 ^e					8.9E-4 ^e			
B	17	1.2E-4	2.5E-4	2.1	9.1E-4	17	1.6E-3	8.5E-4	0.5	3.4E-3
		7.8E-6			1.1E-6		1.2E-3			3.8E-4
		2.7E-5					1.4E-3			
		3.0E-5					1.4E-3			
C	42	4.2E-5	9.1E-5	2.2	5.6E-4	42	1.8E-3	1.0E-3	0.6	6.2E-3
		2.9E-6			3.2E-7		1.3E-3			2.5E-4
		1.3E-5					1.6E-3			
		2.2E-5					1.6E-3			
Vegetated surfaces (B, C)	59	6.5E-5	1.6E-4	2.5	9.1E-4	59	1.7E-3	1.0E-3	0.6	6.2E-3
		3.6E-6			3.2E-7		1.3E-3			2.5E-4
		1.6E-5					1.5E-3			
		2.2E-5					1.6E-3			

^a See Tables 1, 2, 4 and Figures 3 and 4.^b Arithmetic mean.^c Harmonic mean.^d Geometric mean.^e Median.

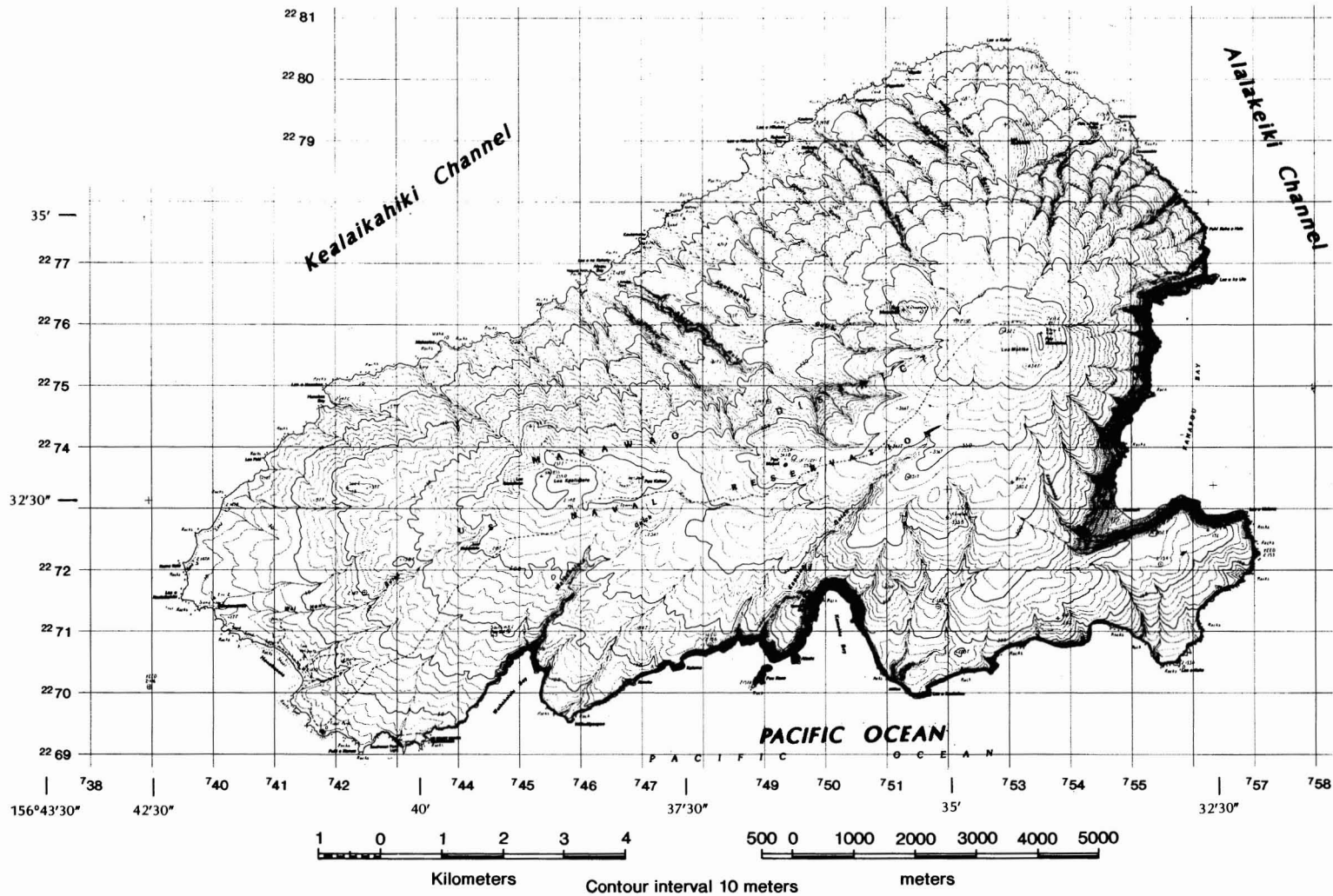


FIGURE 7. Topographic map of Kaho'olawe.

as gleaned from geostatistical analysis (Figure 5), for either the saturated hydraulic conductivity or the sorptivity data. The effort to focus on the area of greatest measurement density was also geostatistically unrewarding (Figure 6). (2) The arithmetic mean values for saturated hydraulic conductivity estimates are smaller (although only slightly) for the vegetated surfaces ($6.5 \times 10^{-5} \text{ m sec}^{-1}$) than for the exposed surface land cover ($9.6 \times 10^{-5} \text{ m sec}^{-1}$); the difference is reversed for the harmonic mean values, 3.6×10^{-6} versus $4.5 \times 10^{-7} \text{ m sec}^{-1}$. (3) The range in saturated hydraulic conductivity estimates for the exposed surface land cover (A) is almost five orders of magnitude; for the other two land covers (B and C) and the combination of B and C (vegetated surfaces), the range is much smaller. (4) There is considerable variability in the saturated hydraulic conductivity estimates for three land covers: coefficients of variation of 6.0, 2.1, and 2.2 for the A, B, and C land

covers, respectively. (5) The average sorptivity values for all three land covers are very similar: 1.0×10^{-3} , 1.6×10^{-3} , and $1.8 \times 10^{-3} \text{ m sec}^{-1/2}$ for the A, B, and C land covers, respectively. (6) The variability in the sorptivity estimates is relatively small for the three land covers: coefficients of variation of 0.5, 0.5, and 0.6 for the A, B, and C land covers, respectively.

RAINFALL-RUNOFF SIMULATIONS

Data

LAND SURFACE. For this study, the island of Kaho'olawe (Figure 7) was divided into 70 catchments (see Figure 8). The segments used to transform the catchments into overland flow planes for the QPBRM simulations are illustrated in Figure 9. The total number of overland flow plane segments

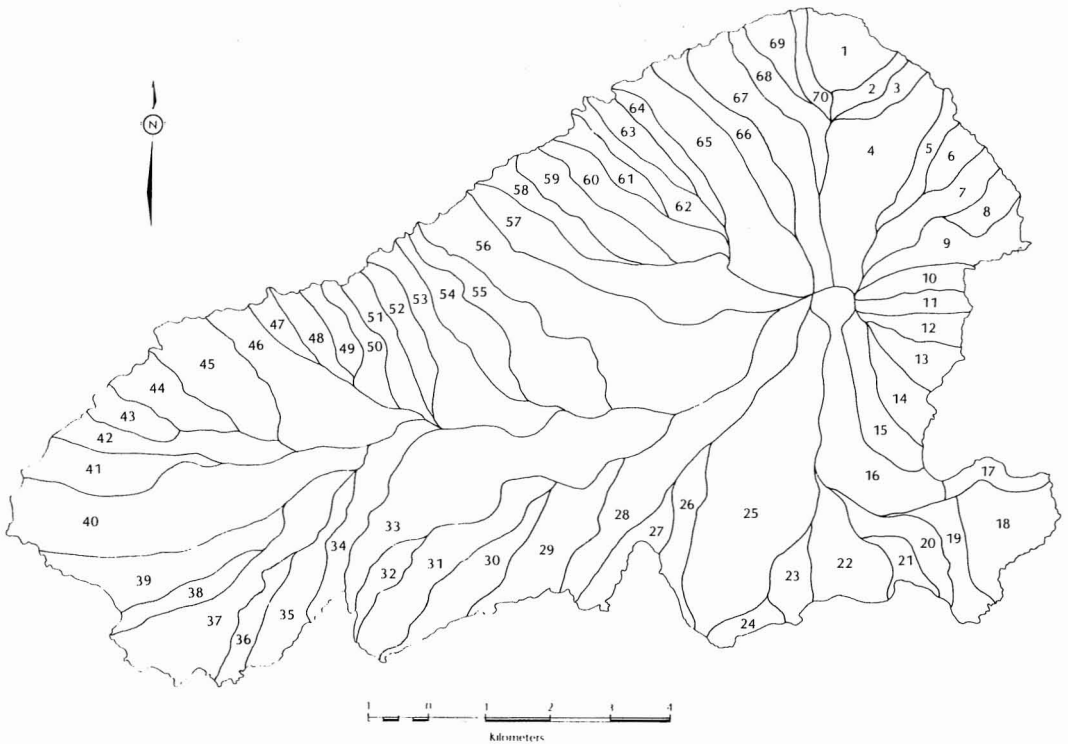


FIGURE 8. Seventy Kaho'olawe catchments. The Hakioawa catchment is no. 4.

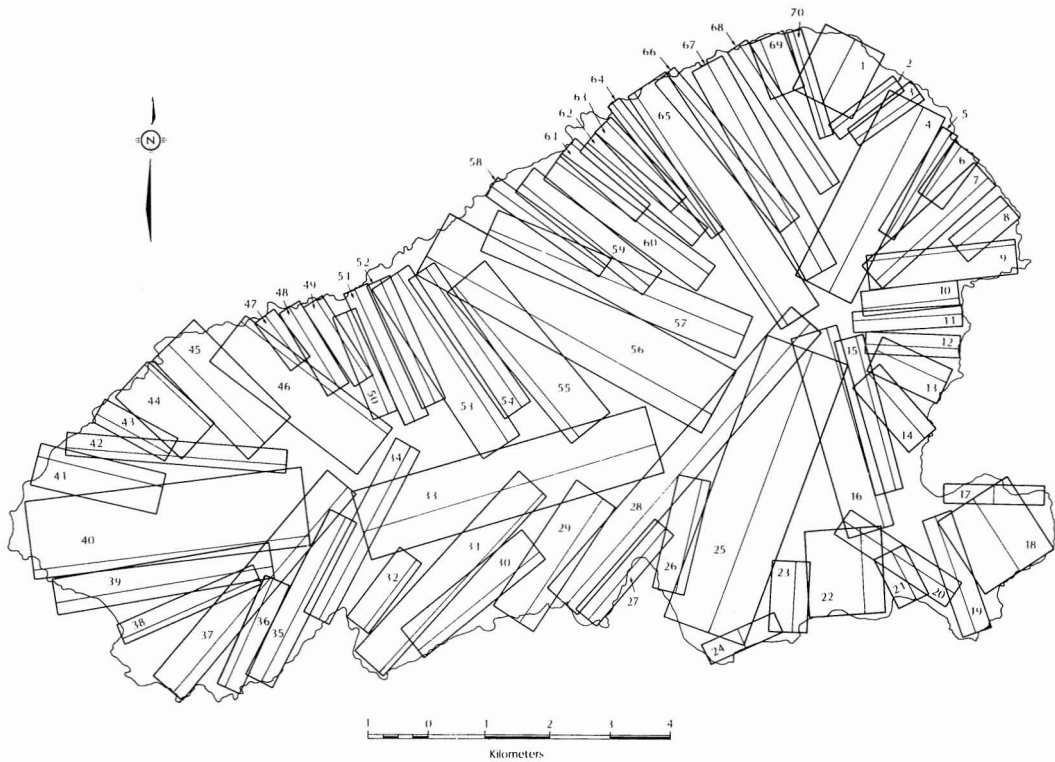


FIGURE 9. Segments used to transform the Kaho'olawe catchments into overland flow planes.

used to represent Kaho'olawe was 1529. The total number of channel reaches for the 70 catchments was 3733. The general characteristics of the Kaho'olawe catchments are summarized in Table 6. Based upon field measurements on the island, a scenario was developed to represent the spatial variability of saturated hydraulic conductivity and sorptivity for Kaho'olawe; the three basic land cover designations in Table 5 are (1) exposed soil or subsoil, (2) shrubs and trees, and (3) grass. This is our distributed (DT) representation. We use the harmonic mean values in Table 5 for saturated hydraulic conductivity and sorptivity for the DT scenario. The harmonic mean is employed in the QPBRM simulations to account for whatever spatial correlation might exist in the measurements of saturated hydraulic conductivity and sorptivity, rather than assume that the measurements are statistically independent as in the standard arithmetic mean. A second scenario

for representing saturated hydraulic conductivity and sorptivity is the average approach, listed in Table 2. Again, we use the harmonic mean values in Table 2 for the saturated hydraulic conductivity and sorptivity for the averaged (AV) scenario. The estimates of initial soil-water content, which varied across Kaho'olawe with land cover, were based upon field TDR measurements; the same values of initial soil-water content were used for each rainfall event because temporal information did not exist. The resulting under- or overestimation of actual soil-water contents for each of the rainfall events was unavoidable because these data were unavailable. The characteristic parameters used for the QPBRM simulations of the Kaho'olawe catchments are given in Table 7. The time step used for all infiltration and flow routing was 120 sec. The space increment for the overland flow segments was 20 m. The average space increment for the open channel flow reaches was

TABLE 6

GENERAL CHARACTERISTICS OF 70 KAHO'OLAWA CATCHMENTS AND REPRESENTATIVE OVERLAND FLOW PLANES

CATCHMENT NO.	AREA		SLOPES (%)		
	M ²	RANK ^a	CHANNEL	LEFT SIDE	RIGHT SIDE
1	1,381,250	31	18.3	1.5	1.5
2	443,750	69	17.2	13.3	3.5
3	475,000	65	15.1	5.7	10.9
4	3,646,875	5	12.1	5.7	7.1
5	684,375	52	15.8	21.8	20.0
6	571,875	63	20.6	24.0	8.6
7	1,268,750	33	14.7	11.8	21.5
8	615,625	61	19.8	8.0	2.0
9	1,453,125	28	16.0	1.5	16.0
10	671,875	53	24.0	9.1	8.9
11	618,750	59	23.6	4.4	4.2
12	646,875	57	25.3	5.5	13.3
13	806,250	47	26.0	7.5	5.5
14	890,625	43	23.4	8.9	6.4
15	1,343,750	32	17.8	8.0	8.7
16	2,956,250	11	12.7	10.0	4.7
17	565,625	64	50.5	22.2	1.3
18	2,028,125	19	13.3	3.5	2.5
19	1,034,375	36	10.1	10.0	22.2
20	993,750	39	10.9	9.2	7.1
21	462,500	66	20.4	2.4	2.7
22	1,784,375	20	12.8	4.2	3.2
23	743,750	49	17.1	3.5	3.9
24	450,000	67	58.0	2.0	2.0
25	7,025,000	1	7.8	3.7	2.6
26	1,006,250	38	17.2	13.3	6.9
27	856,250	44	31.3	7.3	5.3
28	3,612,500	6	7.1	11.2	11.3
29	2,146,875	18	12.4	2.9	4.4
30	1,578,125	22	10.7	5.0	1.7
31	2,478,125	14	6.6	11.4	3.9
32	618,750	59	11.7	7.3	4.9
33	6,065,625	3	5.6	3.8	5.4
34	1,578,125	22	8.6	2.5	2.8
35	1,546,875	24	6.3	4.2	2.9
36	759,375	48	6.8	4.2	3.6
37	3,184,375	9	4.9	11.4	5.2
38	837,500	45	6.0	4.0	5.0
39	2,221,875	17	6.0	5.7	5.7
40	5,815,625	4	4.4	9.2	1.7
41	1,543,750	25	5.2	1.1	2.4
42	1,478,125	27	5.7	8.0	10.9
43	641,667	58	10.0	5.7	2.9
44	1,140,625	34	7.5	3.9	10.0
45	2,303,125	16	8.0	5.2	1.6
46	3,165,625	10	9.4	7.6	13.3
47	434,375	70	10.3	3.1	7.3
48	671,875	53	12.6	4.4	8.0
49	587,500	62	13.3	4.0	4.0
50	815,625	46	12.3	13.3	10.0
51	1,034,375	36	10.1	8.9	8.6
52	937,500	41	9.9	4.2	12.3
53	2,468,750	15	7.6	5.9	15.0
54	1,506,250	26	8.3	7.3	11.8

TABLE 6 (continued)

CATCHMENT NO.	AREA		SLOPES (%)		
	M ²	RANK ^a	CHANNEL	LEFT SIDE	RIGHT SIDE
55	2,875,000	12	7.9	24.0	5.9
56	6,659,375	2	7.6	19.0	4.2
57	3,481,250	8	7.8	10.0	10.0
58	937,500	41	8.6	14.5	5.3
59	1,431,250	30	9.8	24.0	11.4
60	1,706,250	21	11.0	6.9	14.3
61	653,125	56	11.7	10.9	10.0
62	987,500	40	11.6	21.8	18.2
63	709,375	50	12.8	13.3	22.9
64	690,625	51	12.6	17.8	10.7
65	3,556,250	7	10.0	24.6	10.7
66	1,446,875	29	11.4	11.4	18.7
67	2,484,375	13	10.2	13.3	15.0
68	1,109,375	35	13.3	11.1	31.1
69	659,375	55	13.3	5.0	8.4
70	446,875	68	14.7	28.6	13.3

^aFrom largest to smallest.

100 m. No measurements of profile depth were conducted because the prevalence of unexploded ordnance on Kaho'olawe makes it dangerous to dig soil pits. Soil depth was taken as a 1-m (homogeneous) constant for the entire island. It should be noted that the simulated wetting front from the infiltration component of QPBRRM never reached the 1-m depth for any of the events for any of the land covers in this study. Based upon field observations, it is obvious that depression storage does play a role in Kaho'olawe runoff events. For this effort, however, depression storage was set to zero across the en-

tire island because of the absence of field data, thus increasing the magnitude of excess precipitation and simulated runoff. For the runoff generation components of our QPBRRM simulations for Kaho'olawe, we assumed the channel width to be zero, thus reducing the simulated runoff by preventing runoff caused by rainfall falling directly on the channel; this is an acceptable tack because our focus was on the land phase and the generation of overland flow. For each catchment, lateral inflows were routed in channels with constant trapezoidal geometry, because we did not have detailed channel descriptions.

TABLE 7

CHARACTERISTIC PARAMETERS FOR THE KAHO'OLAWA CATCHMENTS FOR THE QPBRRM SIMULATIONS

CATCHMENT	WIDTH, <i>w</i> (m)	MANNING'S ROUGHNESS COEFFICIENT ^a , <i>n</i> (dimensionless)	DEPRESSION STORAGE, <i>D</i> (mm)	PROFILE DEPTH, <i>d</i> (m)
Land cover ^b				
A	—	0.08	0.0	1.0
B	—	0.12	0.0	1.0
C	—	0.16	0.0	1.0
Channel	0	0.05	—	—

^aWoolhiser (1975), French (1985), Engman (1986); $n = n_c$ for channel; $n = n_o$ for overland.

^bSee Table 4 for description.

TABLE 8

CHARACTERISTICS OF THE 10 RAINFALL EVENTS USED IN THE QPBRRM Simulations
OF RAINFALL RUNOFF FOR KAHO'OLAWÉ

EVENT NO.	DATE	MAXIMUM INTENSITY, P_I^a (mm hr ⁻¹)	TOTAL DEPTH, P_D^a (mm)	LENGTH OF EVENT, P_L (hr)
1	6 Feb. 1966	28 (8) ^b	47 (6) ^b	8 (8) ^c
2	23 Apr. 1967	32 (6)	40 (10)	3 (1)
3	3 June 1967	40 (2)	82 (3)	4 (5)
4	16 Jan. 1968	33 (5)	77 (4)	7 (7)
5	16 Apr. 1968	31 (7)	41 (9)	5 (6)
6	3 Oct. 1968	37 (3)	47 (5)	3 (3)
7	16 Jan. 1971	26 (10)	86 (2)	11 (9)
8	31 Dec. 1971	33 (4)	47 (7)	4 (4)
9	23 Jan. 1972	56 (1)	214 (1)	24 (10)
10	1 Sept. 1972	28 (9)	46 (8)	3 (2)

NOTE: These events were recorded at U.S. Weather Service rain gauge station no. 0300 (Hawai'i State Key gauge no. 807) on the leeward side of the island of O'ahu (State of Hawai'i 1973).

^aRounded off to the nearest millimeter.

^bRanking (in parentheses) from largest to smallest.

^cRanking (in parentheses) from shortest to longest.

RAINFALL. The maximum mean annual rainfall near the summit of Kaho'olawe has been estimated to be between 640 and 760 mm per year (State of Hawai'i 1990). The record length and measurement interval for the sparse Kaho'olawe rainfall data are inadequate for abstracting events for our QPBRRM simulations. However, patterns of storm rainfall (U.S. Weather Bureau 1962, Giambelluca et al. 1984) are closely correlated with patterns of mean annual rainfall (Giambelluca et al. 1986) in the Hawaiian Islands. Several years of hourly rainfall data are available for stations on the island of O'ahu. For our study we selected a station on the leeward side of O'ahu as being reasonably representative of the rainfall characteristics for Kaho'olawe; the mean annual rainfall for that U.S. National Weather Service rain gauge (station number 0300) is 820 mm. The 10 rainfall events used to excite QPBRRM for the Kaho'olawe rainfall-runoff simulations in this study are summarized in Table 8 and are graphically illustrated in Figure 10. These 10 events were selected from the largest 25 events occurring over a 6-yr period. Comparison of the maximum rainfall intensities in Table 8 with the saturated hydraulic conductivity (K_s) in Table 5 for the exposed soil and subsoil land cover shows

that the 10 rainfall events will produce excess rainfall for the selected events.

It should be pointed out that we are not simulating observed runoff events in this study (there are no runoff data); therefore, an exact rainfall characterization is not important for our simulations. The 10 rainfall events summarized in Table 8 and shown in Figure 10 are typical (and highly likely) for Kaho'olawe and serve to illustrate the type of Horton runoff response the island experiences during large storms.

Results

The results from the QPBRRM simulations for the entire island of Kaho'olawe are given in Tables 9 through 11. Figure 11 illustrates which catchments experienced runoff for the 10 events. Perusal of the runoff summary variable averages (Q_D , storm flow depth; Q_{pk} , peak stormflow rate) and runoff summaries in Tables 9–11 and Figure 11 leads to the following generalized comments: (1) The distributed representation of saturated hydraulic conductivity (DT) yielded excess precipitation (P_{mx}): (a) for the exposed soil or subsoil (A) land cover for each of the 10 rainfall events, (b) for the shrubs and trees (B) land cover for only two of the 10 rainfall events, and (c) for

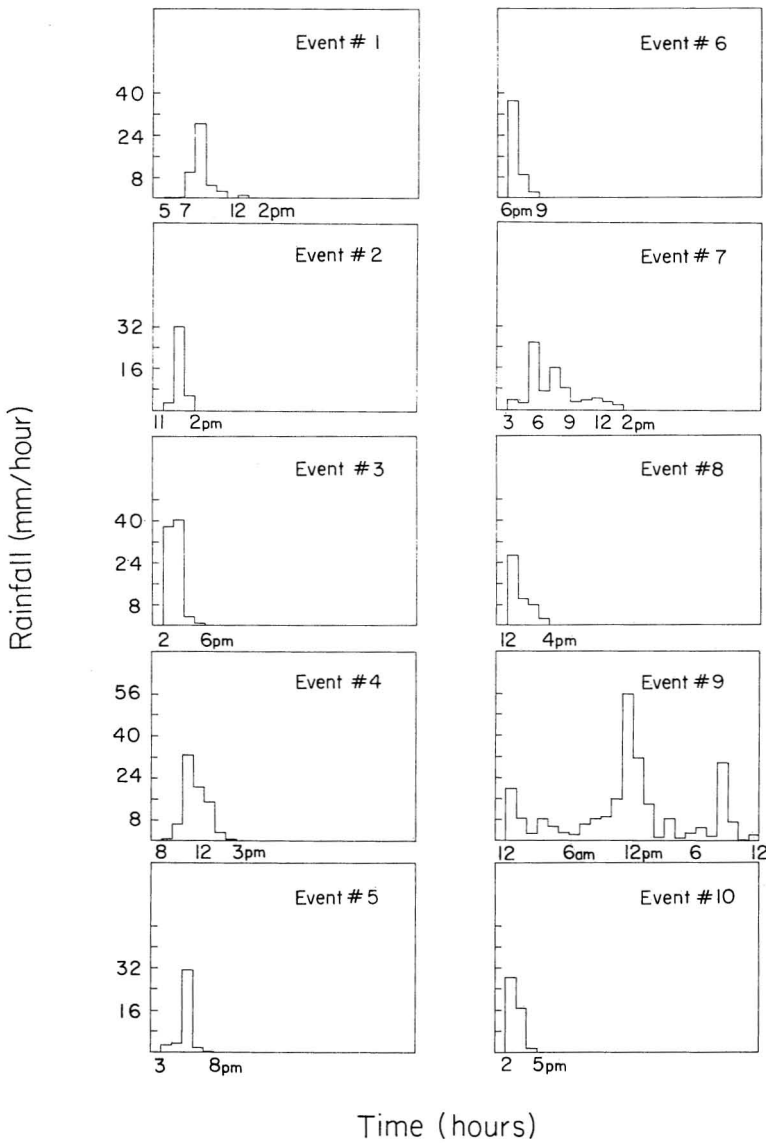


FIGURE 10. Ten rainfall events used for QPBRRM simulations of Horton overland flow on Kaho'olawe.

the grass (C) land cover for eight of the 10 rainfall events. (2) The averaged representation of saturated hydraulic conductivity (AV) yielded excess precipitation (P_{mx}) for eight of the 10 rainfall events. (3) The catchments with the largest response (runoff depth) for the 10 rainfall events were as follows: event 1 (catchment 11), event 2 (catchment 13), event 3 (catchment 11), event 4 (catchment 11), event

5 (catchment 11), event 6 (catchment 70), event 7 (catchment 11), event 8 (catchments 3, 11, 70), event 9 (catchment 11), event 10 (catchment 11). (4) The largest island response was for event 9; the smallest island response was for event 8. (5) The distributed nature of runoff response for the 10 rainfall events corresponded (as was expected) to the land cover distribution.

TABLE 9
 MAXIMUM EXCESS PRECIPITATION (P_{mx}) FOR THE
 QPBRRM SIMULATIONS FOR THE 10 RAINFALL EVENTS
 WITH DISTRIBUTED AND AVERAGED ESTIMATES OF
 SATURATED HYDRAULIC CONDUCTIVITY

EVENT NO.	Distributed, P_{mx} (mm/hr)			Average, P_{mx} (mm/hr)
	LAND COVER			
	A	B	C	
1	17.0	0	8.0	13.0
2	16.6	0	5.6	11.2
3	24.6	0.6	13.6	19.3
4	19.7	0	10.0	15.2
5	18.4	0	8.7	13.9
6	15.3	0	1.6	8.0
7	13.4	0	3.7	8.9
8	5.1	0	0	0
9	49.1	31.4	42.1	46.5
10	6.7	0	0	0

The results thus far have been interpreted on an island-wide basis. We now turn to the Hakioawa catchment (no. 4 in Table 10 and Figure 8) to facilitate a closer inspection of the impact of land cover variability on runoff response at the catchment scale. Figures 12 and 13 show the Hakioawa catchment, the land cover distribution, and the overland flow planes used to approximate the catchment for the QPBRRM simulations. Figure 14 illustrates the distribution of excess rainfall, reinfiltration (runon), and contributing overland flow partial source areas for the 10 events. Table 12 reports QPBRRM simulation results for distributed (DT) and averaged (AV) estimates of saturated hydraulic conductivity and sorptivity for the 10 rainfall events. Table 13 shows the runoff contributions of the Hakioawa overland flow plane segments for the 10 rainfall events for the alternative representations of near-surface soil hydraulic properties. One should keep in mind that we could have focused our attention on any of the 70 Kaho'olawe catchments. We selected Hakioawa because it exhibits considerable land cover variability, has areas of substantial observed erosion, and was the focus of much of our field investigation.

Inspection of Figure 14 and Tables 12 and

13 leads to the following generalized comments: (1) The areas of excess rainfall, reinfiltration, and Hortonian overland flow corresponded to the distribution of land cover. (2) The averaged representation of saturated hydraulic conductivity (versus the distributed representation) yielded greater runoff response (Q_D) for seven of the 10 rainfall events and larger peak flows (Q_{PK}) for eight of the 10 events. (3) The hydrologic response of the upper three channel reaches of the Hakioawa catchment was greater with the distributed representation (DT) of saturated hydraulic conductivity. The hydrologic response of the lower three channel reaches of the Hakioawa catchment was greater with the averaged representation (AV) of saturated hydraulic conductivity. For channel reaches 6, 7, and 12, the greater response varied between the DT and AV representations of saturated hydraulic conductivity depending upon the rainfall event. (4) The averaged representation (AV) of saturated hydraulic conductivity resulted in substantial overestimates in total runoff from the catchment and misrepresented (relative to the DT estimates) the distribution and timing of surface runoff within the catchment. (But note that this statement is made in the absence of field observations.) (5) Runoff response was a sensitive nonlinear function of rainfall depth, intensity, and timing and land cover distribution. Rainfall events of similar depth but different distribution led to quite different runoff response (e.g., events 1, 6, and 8).

DISCUSSION

The field study undertaken was highly successful, providing a new and unique data set of near-surface soil hydraulic property information for Kaho'olawe. The large variability (within and between land covers) and uncertainty in the saturated hydraulic conductivity data provide physically based process evidence that hydrologic response is extremely variable on Kaho'olawe. It was not possible in this study to do any spatial interpolation of the Kaho'olawe data with geostatistical methods (kriging) because there was no

TABLE 10

RUNOFF DEPTH (mm) FOR THE 70 KAHŌ'OLAWĒ CATCHMENTS FOR QPBRRM SIMULATIONS WITH THE DISTRIBUTED REPRESENTATION OF SATURATED HYDRAULIC CONDUCTIVITY (DT) FOR THE 10 RAINFALL EVENTS

CATCHMENT ^d NO.	EVENT NO.									
	1	2	3	4	5	6	7	8	9	10
1	0	0	~ 0.0 ^b	0	0	0	0	0	32.6	0
2	0	0.8	1.8	2.0	2.9	0.2	4.3	~ 0.0	49.7	~ 0.0
3	1.8	1.5	3.4	3.8	1.9	0.5	2.0	0.1	54.2	0.1
4	3.2	2.0	5.9	7.4	3.2	0.4	2.4	~ 0.0	44.5	~ 0.0
5	4.0	2.4	7.6	7.4	4.2	0.8	2.8	~ 0.0	66.9	0.1
6	1.1	1.0	1.9	2.3	1.1	0.3	1.3	~ 0.0	44.1	~ 0.0
7	5.5	3.5	9.9	10.7	5.6	1.1	4.6	~ 0.0	67.6	0.1
8	0.9	0.7	1.8	2.1	1.0	0.2	1.0	~ 0.0	45.5	~ 0.0
9	2.7	1.9	5.4	0.5	2.7	0.4	2.8	~ 0.0	58.9	0.1
10	5.4	3.6	10.2	11.0	5.5	0.8	4.4	~ 0.0	71.4	0.1
11	9.7	2.6	18.4	20.3	10.1	2.6	10.6	0.1	97.2	0.3
12	5.4	4.2	10.8	11.2	5.6	1.4	5.5	~ 0.0	70.8	0.2
13	8.0	6.3	15.4	17.1	8.2	1.8	8.6	~ 0.0	77.2	0.2
14	4.5	0.1	8.7	9.6	4.6	1.0	4.8	~ 0.0	56.0	0.1
15	5.6	4.0	10.8	11.1	5.6	1.1	5.0	~ 0.0	62.9	0.1
16	5.9	4.3	10.4	12.9	6.1	1.0	6.0	~ 0.0	55.7	0.1
17	0.2	~ 0.0	0.4	0.5	0.2	~ 0.0	~ 0.0	0	31.4	0
18	0.7	0.5	1.6	1.8	0.7	0.1	0.7	~ 0.0	34.9	~ 0.0
19	4.2	3.2	7.8	8.3	4.4	1.1	4.2	~ 0.0	56.8	0.1
20	2.4	1.7	5.6	5.2	2.5	0.6	2.3	~ 0.0	57.5	0.1
21	6.3	4.9	12.2	14.0	6.4	1.2	6.8	~ 0.0	77.3	0.1
22	5.8	4.4	10.8	13.4	5.9	0.9	6.4	~ 0.0	48.6	0.1
23	6.4	4.9	12.7	14.2	6.6	1.2	6.8	~ 0.0	71.5	0.1
24	0	0	~ 0.0	0	0	0	0	0	32.3	0
25	4.4	3.2	9.1	11.1	4.5	0.6	4.7	~ 0.0	46.7	~ 0.0
26	5.8	4.2	11.4	12.1	1.2	1.2	5.4	~ 0.0	63.9	0.1
27	1.2	0.9	2.2	2.5	1.2	0.3	1.3	~ 0.0	47.8	~ 0.0
28	4.4	3.1	8.6	8.6	4.6	0.7	3.8	~ 0.0	56.9	0.1
29	1.0	0.7	2.6	2.6	1.0	0.1	0.9	~ 0.0	39.1	~ 0.0
30	2.3	1.7	4.6	5.4	2.3	2.4	2.5	~ 0.0	51.7	~ 0.0
31	2.9	2.2	5.7	6.8	3.0	0.5	3.2	~ 0.0	50.2	0.1
32	0.3	0.1	0.9	0.6	0.3	0	0.1	0	46.5	0
33	5.0	3.8	9.5	11.3	5.1	0.7	5.3	~ 0.0	46.2	0.1
34	6.5	5.1	12.5	14.2	6.7	1.3	7.0	~ 0.0	78.1	0.1
35	1.4	1.0	2.7	3.2	1.5	0.3	1.4	~ 0.0	50.4	~ 0.0
36	0.5	0.1	1.2	1.2	0.5	~ 0.0	0.1	0	50.0	0
37	0.8	0.6	1.3	1.7	0.9	0.2	0.9	~ 0.0	38.6	~ 0.0
38	~ 0.0	~ 0.0	~ 0.0	~ 0.0	~ 0.0	0	~ 0.0	0	45.0	0
39	~ 0.0	~ 0.0	0.1	0.1	~ 0.0	0	~ 0.0	0	38.7	0
40	0.3	0.2	0.6	0.7	0.3	~ 0.0	0.3	~ 0.0	24.1	~ 0.0
41	~ 0.0	~ 0.0	~ 0.0	~ 0.0	~ 0.0	0	~ 0.0	0	35.7	0
42	0.3	0.2	0.5	0.6	0.3	0.1	0.3	~ 0.0	46.0	~ 0.0
43	0	0	0	0	0	0	0	0	41.7	0
44	0	0	0	0	0	0	0	0	31.2	0
45	0	0	0	0	0	0	0	0	27.1	0
46	1.2	1.0	2.2	2.4	1.3	0.3	1.3	~ 0.0	27.7	~ 0.0
47	2.1	1.7	4.1	4.4	2.2	0.6	2.3	~ 0.0	53.2	0.1
48	1.9	1.6	3.5	3.8	2.0	0.6	2.1	~ 0.0	80.0	0.1
49	0	0	0	0	0	0	0	0	44.1	0
50	2.5	2.1	4.5	5.3	2.6	0.7	2.8	~ 0.0	53.8	0.1
51	1.7	1.4	3.2	3.5	1.8	0.5	1.9	~ 0.0	52.6	0.1
52	1.1	0.9	2.1	2.3	1.1	0.3	1.2	~ 0.0	49.5	~ 0.0
53	4.5	3.4	8.0	9.4	4.6	0.9	4.6	~ 0.0	52.0	0.1

TABLE 10 (continued)

CATCHMENT ^a NO.	EVENT NO.									
	1	2	3	4	5	6	7	8	9	10
54	0.9	0.7	1.5	1.8	0.9	0.2	0.9	~ 0.0	45.4	~ 0.0
55	1.6	1.2	2.5	3.1	1.7	0.4	1.5	~ 0.0	34.4	0.1
56	2.0	1.2	3.6	4.7	2.0	0.2	1.5	~ 0.0	31.8	~ 0.0
57	3.0	2.3	5.5	6.2	3.0	0.7	3.1	~ 0.0	46.6	0.1
58	1.5	1.0	3.3	3.1	1.6	0.3	1.3	~ 0.0	53.7	~ 0.0
59	1.2	1.0	2.1	2.3	1.2	0.4	1.3	~ 0.0	40.4	0.1
60	0.1	~ 0.0	0.4	0.2	0.1	0	0	0	44.1	0
61	0	0	~ 0.0	0	0	0	0	0	48.1	0
62	1.0	0.8	1.9	2.1	1.1	0.3	1.1	~ 0.0	50.2	~ 0.0
63	0	0	~ 0.0	0	0	0	0	0	40.3	0
64	0.2	~ 0.0	0.4	0.4	0.2	0	~ 0.0	0	52.1	0
65	4.4	3.1	7.0	8.8	4.5	0.8	4.0	~ 0.0	41.3	0.1
66	2.2	0.8	4.4	3.9	2.2	~ 0.0	0.6	0	57.4	0
67	2.2	1.4	4.2	4.5	2.2	0.4	1.8	~ 0.0	49.9	~ 0.0
68	2.8	2.0	5.3	5.3	2.9	0.7	2.5	~ 0.0	56.1	0.1
69	0.8	0.7	1.4	1.7	0.8	0.2	0.9	0	38.8	~ 0.0
70	3.5	2.9	6.4	6.9	3.7	1.2	3.9	0.1	66.9	0.2

^a See Figure 8 for location.

^b If runoff depth < 0.05 mm, denoted as ~ 0.0.

TABLE 11

TOTAL RAINFALL AND RUNOFF FOR THE 70 KAHŌ'OLAWÉ CATCHMENTS FOR THE QPBRM SIMULATIONS WITH THE DISTRIBUTED REPRESENTATION OF SATURATED HYDRAULIC CONDUCTIVITY (DT) FOR THE 10 RAINFALL EVENTS

EVENT NO.	RAINFALL (m ³)	RUNOFF (m ³)	% HORTON RESPONSE ^a
1	5,472,318	302,850	5.5
2	4,657,292	213,333	4.6
3	9,547,448	574,075	6.0
4	8,965,286	652,731	7.3
5	4,773,724	306,773	6.4
6	5,472,318	67,567	1.2
7	10,013,177	298,065	3.0
8	5,472,318	1,366	0.02
9	24,916,511	5,270,084	21.2
10	5,355,885	6,293	0.1
Mean	8,464,628	769,314	—
Standard deviation	6,138,496	1,596,376	—
Coefficient of variation	0.7	2.1	—

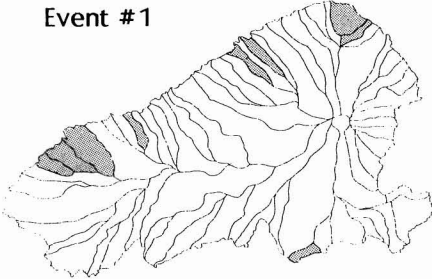
^a Rounded off to 1/10 of a percent.

structure in the near-surface soil hydraulic property data. An explanation for the lower saturated hydraulic conductivity values (in some instances) on Kaho'olawe for the vegetated surface than for the exposed soil and subsoil surfaces is the cracks in the exposed surfaces, which are common (see Table 4 footnote). The study illustrates that parameter surface maps are difficult to generate, based upon geostatistical techniques, for near-surface soil hydraulic properties at the insular scale with limited data. The saturated hydraulic conductivity and sorptivity data reported here facilitated the simulation of rainfall-runoff response for Kaho'olawe for events of different sizes with a quasi-physically based rainfall-runoff model of Hortonian overland flow.

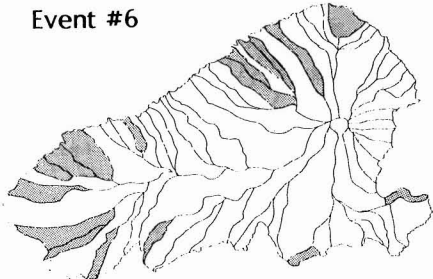
The runoff estimates reported here, based upon physically based rainfall-runoff event simulations, provide an improved hydrologic response characterization for Kaho'olawe. The runoff response for the 10 large rainfall

FIGURE 11. Kaho'olawe catchments "not" experiencing runoff (shaded) for the 10 rainfall events used in QPBRM simulations.

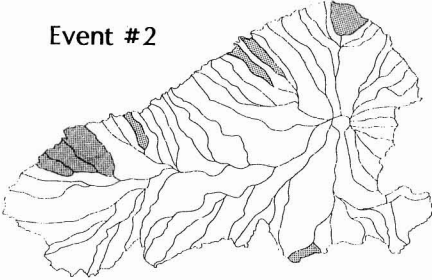
Event #1



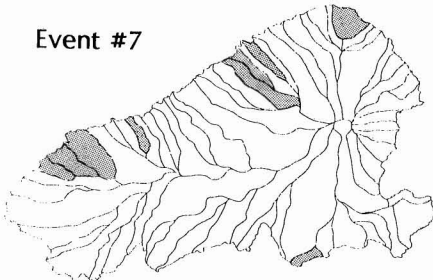
Event #6



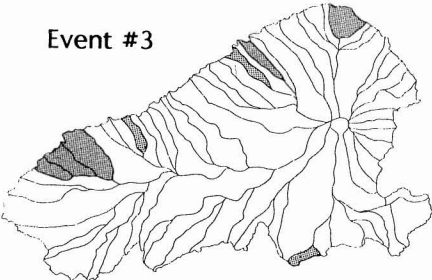
Event #2



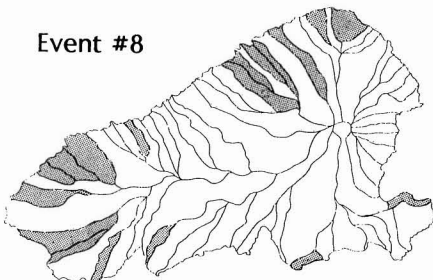
Event #7



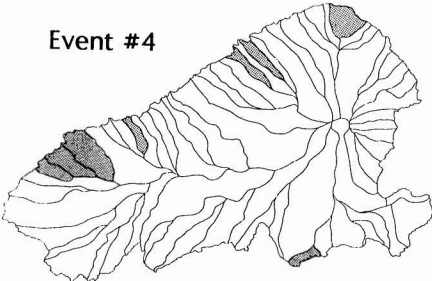
Event #3



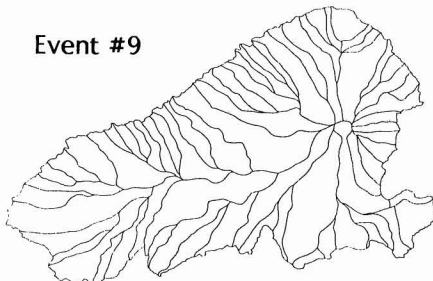
Event #8



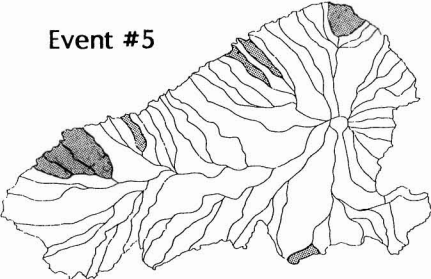
Event #4



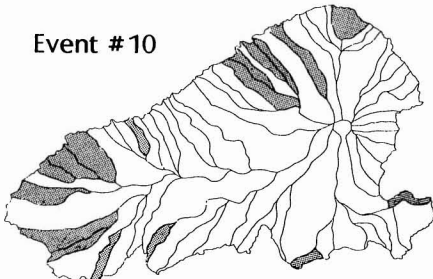
Event #9



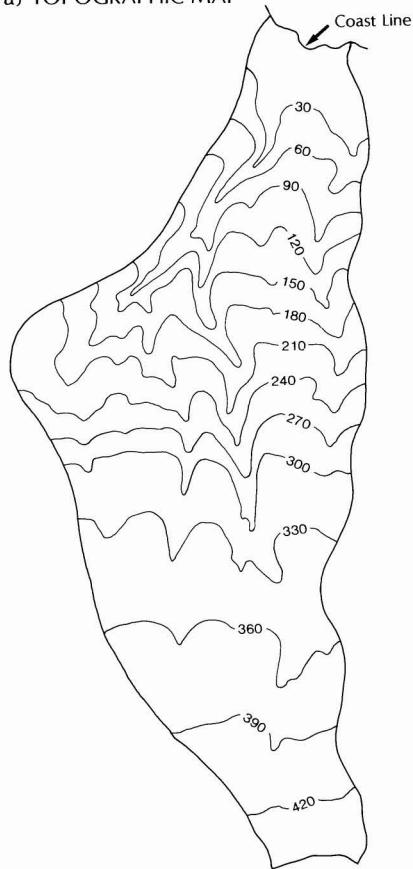
Event #5



Event #10

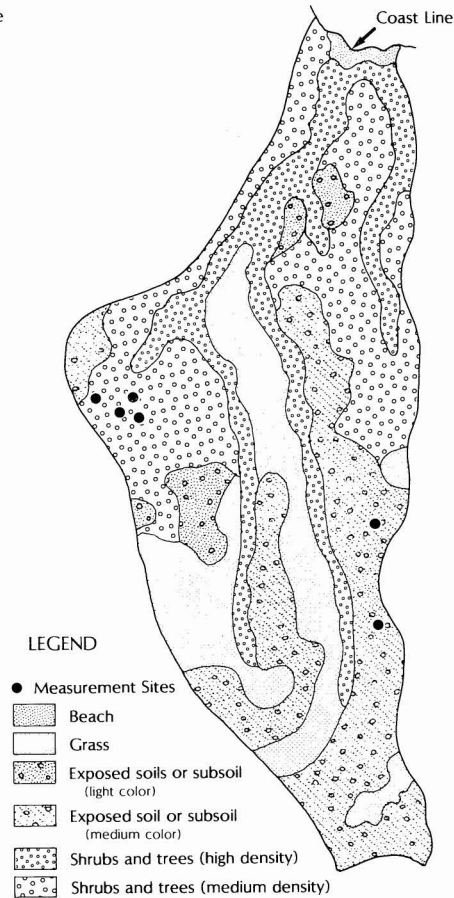


a) TOPOGRAPHIC MAP



Contour Interval = 30 meters

b) LANDCOVER MAP



LEGEND

- Measurement Sites
- Beach
- Grass
- Exposed soils or subsoil (light color)
- Exposed soil or subsoil (medium color)
- Shrubs and trees (high density)
- Shrubs and trees (medium density)

c) OVERLAND FLOW PLANE MAP

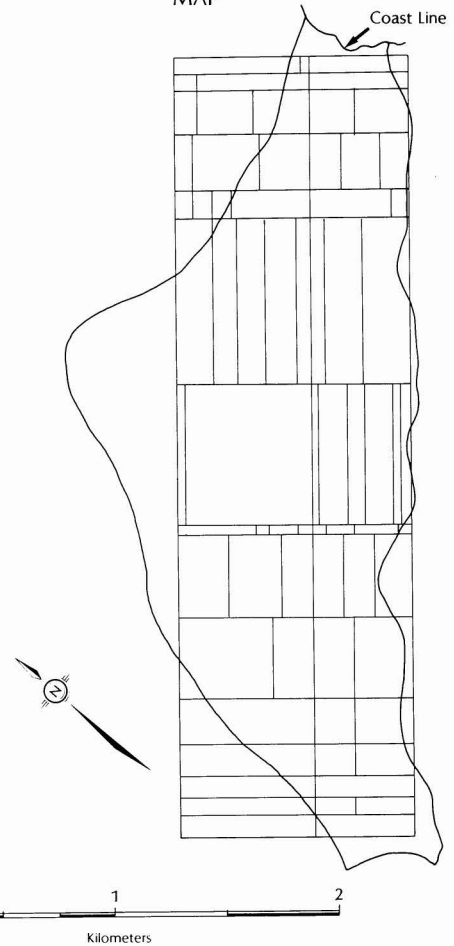
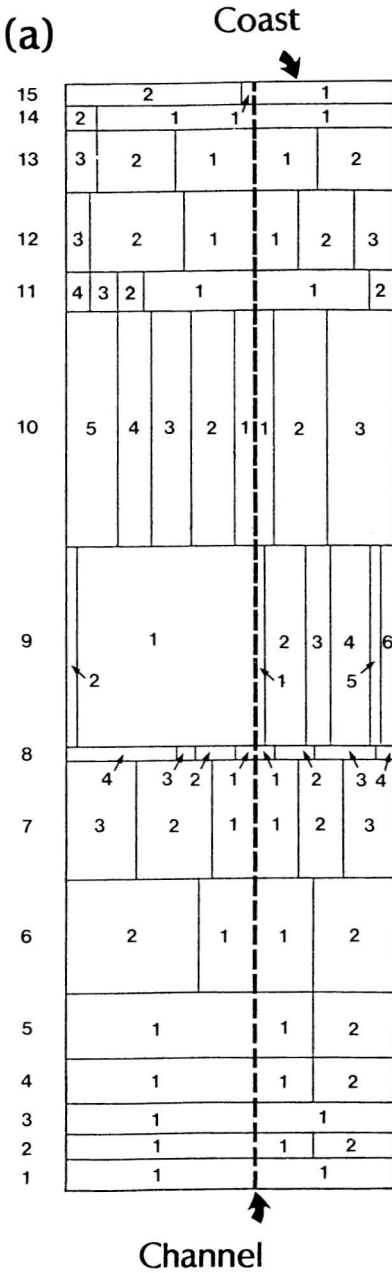
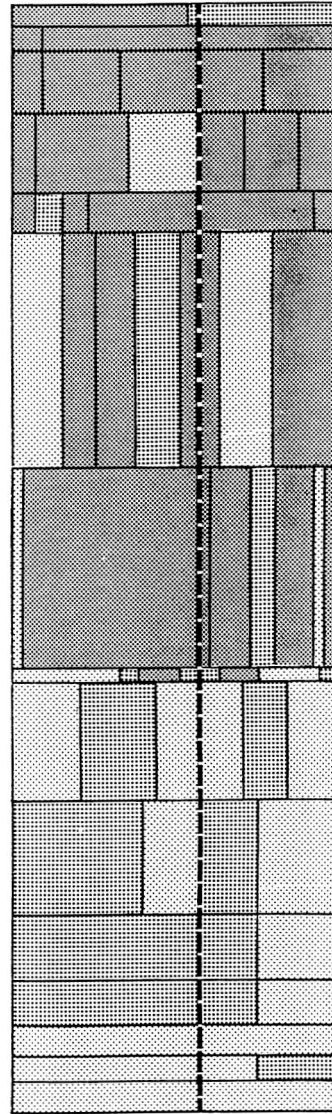


FIGURE 12. Hakioawa catchment: (a) topography, (b) land cover distribution, and (c) overland flow planes.



(b) LAND COVER




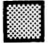

-  Exposed soil/subsoil (a)
-  Shrubs/trees
-  Grass (C)

FIGURE 13. Hakioawa catchment, no. 4 on Figure 8: (a) overland flow plane and channel segment numbers, and (b) land cover characterization.

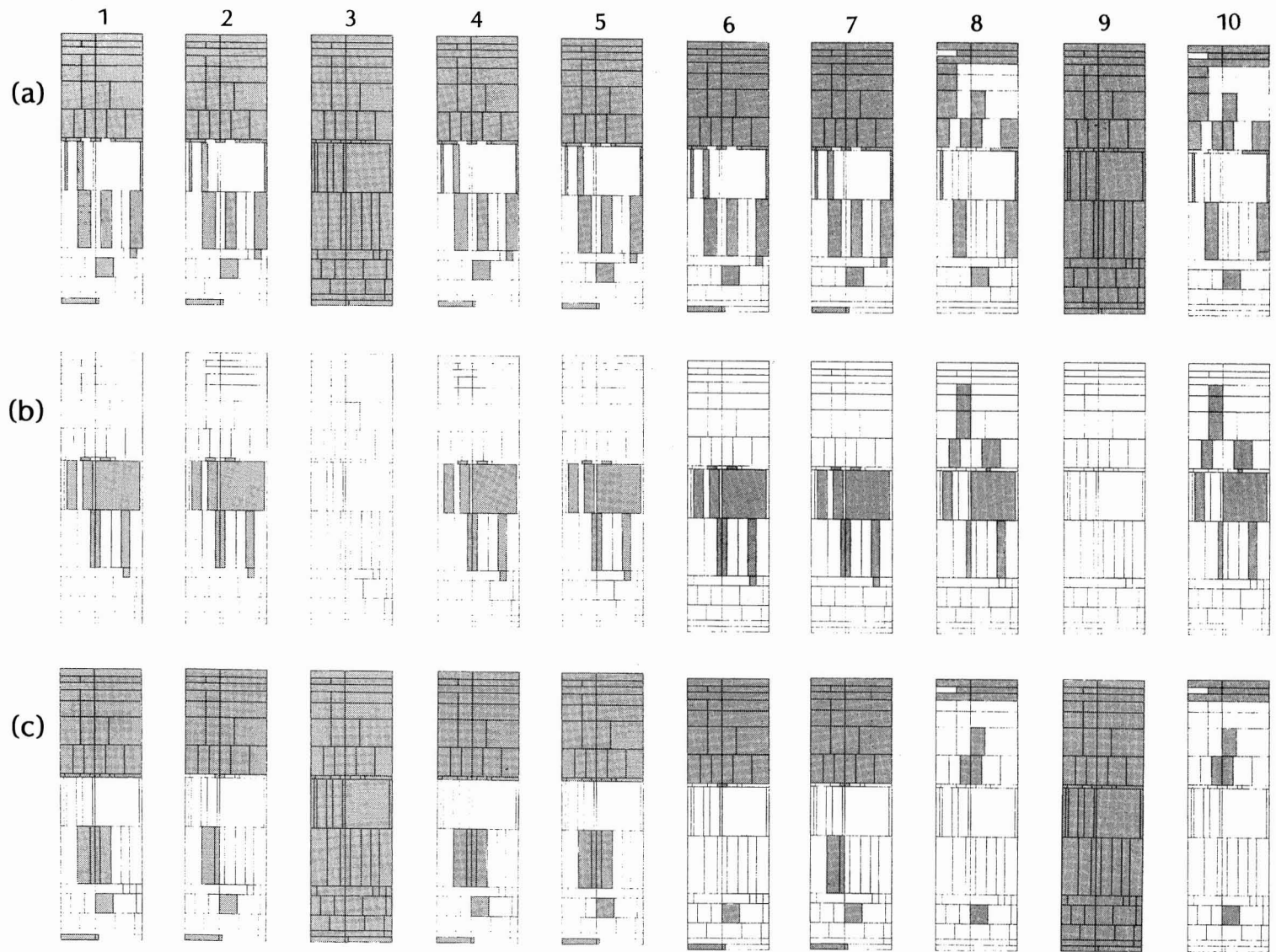


FIGURE 14. Hydrologic response (shaded) for the Hakoawa catchment for the 10 rainfall events: (a) overland flow plane segments experiencing excess rainfall, (b) overland flow plane segments experiencing infiltration, and (c) overland flow segments that are partial source areas. The bottom edge of each response representa-

TABLE 12

RUNOFF SUMMARY VARIABLES FOR THE QPBRRM SIMULATIONS FOR THE 10 RAINFALL EVENTS FOR THE HAKIOAWA CATCHMENT WITH DISTRIBUTED AND AVERAGED ESTIMATES OF SATURATED HYDRAULIC CONDUCTIVITY AND SORPTIVITY

EVENT NO.	DISTRIBUTED, K_s		AVERAGE, K_s	
	Q_D (mm) ^a	Q_{PK} (LS ⁻¹)	Q_D (mm) ^a	Q_{PK} (LS ⁻¹)
1	3.2	4,145	6.4	8,210
2	2.1	2,428	2.4	3,633
3	5.9	5,986	11.1	15,039
4	7.4	5,389	16.1	10,891
5	3.2	4,375	6.1	8,418
6	0.4	629	0.1	59
7	2.4	1,921	2.9	3,321
8	0.01	13	0	0
9	44.5	23,961	66.3	34,395
10	0.04	53	0	0
Mean	6.9	4,890	11.1	8,397
Standard deviation	13.4	7,041	20.1	10,463
Coefficient of variation	1.9	1.4	1.8	1.2

^aRounded off to 0.1 mm.

events is much smaller than the qualitative estimate illustrated in Figure 2. One should note, however, that 20% surface runoff is considerable for the near-surface hydrogeologic conditions typical of Hawai'i. To improve upon the simulations in this study will require better estimates of rainfall variability across the island and evapotranspiration estimates between events for estimates of spatially variable event antecedent soil-water contents. Runoff simulations of the type reported here combined with evapotranspiration estimates could be used in a near-surface water balance to characterize, by difference, recharge, which could in turn be used to estimate soil-water contents in space and time for Kaho'olawe. Information on potentially available soil-water content would be extremely useful for future revegetation efforts on Kaho'olawe.

Paradise Lost or Restoration Geomorphology?

The work reported in this paper sets a foundation for an ongoing effort concerned with simulating sediment transport on Kaho'olawe. Inspection of Figure 11 shows that even for the smallest of the 10 simulated rainfall-runoff events most of the Kaho'olawe

catchments experienced overland flow and, therefore, are potentially vulnerable to erosion; for event 9 the entire island was vulnerable. Inspection of Figure 14 illustrates, on a smaller scale, the potential location of sediment sources and deposition sites for the Hakioawa catchment for the 10 events; the excess rainfall locations are taken here as a surrogate for sediment sources, and the re-infiltration locations are taken here as a surrogate for deposition sites. The distribution of runoff-producing areas shown in Figure 14 agrees well with our field observations of erosion surfaces for the Hakioawa catchment and thus provides some confidence in the QPBRRM simulations. In future work we plan to carefully map partial source areas during large rainfall-runoff events; this much-needed information will be used to evaluate model performance.

The QPBRRM simulations of surface runoff by the Horton mechanism enable us to estimate the velocities and depths of overland flow for different land covers, which can be coupled to a process-based erosion model. The sediment load from an upland source is controlled by the amount of sediment made available for transport by detachment processes and by the transport capacity of the

TABLE 13

RUNOFF FROM OVERLAND FLOW PLANE SEGMENTS FOR EACH CHANNEL REACH OF THE HAKIOAWA CATCHMENT
FOR THE 10 RAINFALL EVENTS FOR DISTRIBUTED^a (DT) AND AVERAGED^a (AV) REPRESENTATIONS OF SATURATED HYDRAULIC CONDUCTIVITY AND SORPTIVITY

CHANNEL REACH NO. ^b	RUNOFF (m ³)																			
	EVENT 1		EVENT 2		EVENT 3		EVENT 4		EVENT 5		EVENT 6		EVENT 7		EVENT 8		EVENT 9		EVENT 10	
	DT	AV	DT	AV	DT	AV	DT	AV	DT	AV	DT	AV	DT	AV	DT	AV	DT	AV	DT	AV
1	1,224	801	1,022	346	1,885	1,298	2,665	1,725	1,196	779	218	10	1,411	402	4	0	6,861	6,362	18	0
2	789	592	635	245	1,261	977	1,768	1,358	793	573	147	8	873	288	3	0	4,931	4,835	14	0
3	1,224	801	1,022	346	1,885	1,298	2,665	1,725	1,196	779	218	10	1,411	402	4	0	6,861	6,362	18	0
4	504	849	174	304	1,070	1,512	1,339	2,279	494	796	<1	7	155	362	0	0	9,593	11,537	0	0
5	720	1,212	248	434	1,529	2,160	1,913	3,255	706	1,137	1	10	221	517	0	0	13,705	16,481	0	0
6	2,185	2,316	1,244	925	4,431	4,068	5,347	5,980	2,196	2,202	274	27	1,472	1,080	7	0	22,212	23,172	30	0
7	2,959	2,564	1,635	957	5,229	4,455	7,253	6,407	2,918	2,423	511	39	2,124	1,133	15	0	20,393	21,806	63	0
8	121	290	9	105	358	495	348	679	120	277	<1	2	4	128	0	0	2,056	2,715	0	0
9	0	4,201	0	1,495	1	7,360	0	10,691	0	3,969	0	44	0	1,798	0	0	19,873	46,801	0	0
10	955	4,974	493	1,833	2,359	8,667	1,766	12,388	1,005	4,721	0	51	368	2,183	0	0	29,056	49,522	0	0
11	0	780	0	290	<1	1,371	0	1,998	0	740	0	8	0	344	0	0	3,739	8,487	0	0
12	783	1,653	633	651	1,493	2,865	1,649	4,064	811	1,581	203	20	850	764	5	0	9,583	15,451	20	0
13	0	1,324	0	483	<1	2,316	0	3,344	0	1,255	0	14	0	576	0	0	6,551	15,297	0	0
14	0	530	0	193	<1	926	0	1,338	0	502	0	6	0	230	0	0	2,621	6,119	0	0
15	85	492	9	166	152	877	226	1,315	79	461	<1	4	7	200	0	0	4,230	6,764	0	0
Total runoff	11,549	23,379	7,124	8,773	21,654	40,645	26,939	58,546	11,514	22,195	1,574	260	8,896	10,407	38	0	162,265	241,711	163	0

^a See Tables 4 and 2 (respectively) for characterization of distributed and averaged saturated hydraulic conductivity and sorptivity values.

^b See Figure 13a.

transport agent. Simulation of human time scale landscape evolution scenarios, under different management options, by coupling our QPBRRM simulations to an erosion model should be useful in the restoration of Kaho'olawe. To complete our erosion simulations, we will make field measurements of detachment and sediment transport rates for the different land covers.

CONCLUSIONS

Overland flow by the Horton mechanism, resulting from overgrazing and military activity, has led to substantial erosion problems on the Hawaiian island of Kaho'olawe. In this paper we present preliminary simulations of runoff-producing areas for the entire island of Kaho'olawe based upon a physically based rainfall-runoff event model. Our results indicate, for 10 large rainfall events, that surface runoff by the Horton mechanism can be as great as 20% of rainfall. This amount of runoff, although large for Hawai'i, is much smaller than the prior estimate of 75% by a qualitative water-balance approach. Our results identify partial source areas of overland flow, where runoff is generated, that are important for erosion. In this ongoing effort we are currently linking our near-surface hydrologic simulations with a physically based erosion model to investigate the past and future evolution of the Kaho'olawe landscape on a human time scale, which will be useful in future restoration activities.

ACKNOWLEDGMENTS

In Hawai'i there is a tremendous *aloha 'āina*, "love of the land." The work described here could not have been undertaken without the invitation and cooperation of the Protect Kaho'olawe 'Ohana (PKO). We are grateful to the PKO members who helped us organize the two Kaho'olawe accesses. The first access team was Rod Adlawan (O'ahu), Tom Giambelluca (O'ahu), Dan Holmes (Maui), Kim Kanoa (O'ahu), Keith Loague (California), Kalani Pruzt (O'ahu), Craig Rowland (O'ahu), Burt Sakata (Maui), and Ste-

ven Vana (O'ahu). The second access team was Fiona Dempster (O'ahu), Tom Giambelluca (O'ahu), Dan Holmes (Maui), Mike Kamaka (O'ahu), Kim Kanoa (O'ahu), Rose King (O'ahu), Keith Loague (California), Richard Miller (O'ahu), Mike Parke (O'ahu), Dave Penn (O'ahu), Kalikiano Bal (Maui), and Burt Sakata (Maui). The U.S. Navy supported us on both of our accesses; in particular we would like to thank Lieutenant Vernon Young (O'ahu) for his assistance. We are also grateful to Dick Green from the University of Hawai'i for the loan of equipment on the second access. The land cover map was generated by Yuan Qing Li, Fang Tao, and Yuhao Wang from the Department of Geography at the University of Hawai'i. The figures were drafted by Gord Hodge (Courtenay, British Columbia, Canada) and Frank Murillo (California). We also wish to extend our heartfelt *mahalo nui loa* to Keoni Fairbanks (Maui), Davianna McGregor (O'ahu), Ricky Apana (Maui), Robert Lu'uwai (Maui), Rendell Tong (O'ahu), Hardy Spoehr (O'ahu), and Uncle Les Kuloloio (Maui), for their awesome assistance. The effort reported here was principally supported by the Kaho'olawe Island Conveyance Commission, established by the U.S. Congress. Much of the preparation of the first draft of the manuscript was completed during K.L.'s "Parker Mission" trip to Japan (July 1993), which was sponsored by the Hokkaido River Disaster Prevention Research Center.

LITERATURE CITED

- ALLEN, M. S. 1987. Kaho'olawe archaeological materials. Appendix A in P. Rosendahl, A. Haun, J. Halbig, M. Kaschko, and M. S. Allen, Draft Report Kaho'olawe Excavations, 1982-3, Data Recovery Project, Island of Kaho'olawe, Hawai'i. Paul H. Rosendahl, Ph.D., Inc. Prepared for Department of the Navy, Pacific Division, Naval Facilities Engineering Command, Pearl Harbor, Hawai'i.
- ARMSTRONG, R. W. (ED.). 1983. Atlas of Hawaii, 2nd ed. University of Hawai'i Press, Honolulu.

- DALTON, F. N. 1992. Development of time-domain reflectometry for measuring soil water content and bulk soil electrical conductivity. Pages 143–167 in G. C. Topp, W. D. Reynolds, and R. E. Green, eds. *Advances in measurement of soil physical properties: Bringing theory into practice*. Soil Sci. Soc. Am. Spec. Publ. 30.
- DUNNE, T. 1978. Field studies of hillslope flow processes. Pages 227–293 in M. J. Kirkby, ed. *Hillslope hydrology*. Wiley-Interscience, New York.
- ENGMAN, E. T. 1974. A partial area model for simulating surface runoff from small watersheds. Ph.D. diss., Pennsylvania State University, University Park.
- . 1986. Roughness coefficients for routing surface runoff. *J. Irrig. Drain. Eng.* 112: 39–53.
- FREEZE, R. A. 1980. A stochastic-conceptual analysis of rainfall-runoff processes on a hillslope. *Water Resour. Res.* 16: 391–408.
- FRENCH, R. H. 1985. *Open-channel hydraulics*. McGraw Hill, New York.
- GIAMBELLUCA, T. W., L. S. LAU, Y.-S. FOK, and T. A. SCHROEDER. 1984. Rainfall frequency study for Oahu. Rep. R-73. Department of Land and Natural Resources, Division of Water and Land Development, State of Hawai'i, Honolulu.
- GIAMBELLUCA, T. W., M. A. NULLET, and T. A. SCHROEDER. 1986. Rainfall atlas of Hawaii. Rep. R-82. Department of Land and Natural Resources, Division of Water and Land Development, State of Hawai'i, Honolulu.
- GREEN, R. E., L. R. AHUJA, S. K. CHONG, and L. S. LAU. 1982. Water conduction in Hawaii oxic soils. *Water Resource Research Center Tech. Rep.* 143. University of Hawai'i, Honolulu.
- KAHO'OLAWA ISLAND CONVEYANCE COMMISSION. 1993. *Kaho'olawe Island: Restoring a cultural treasure*. Final report to the Congress of the United States. Kaho'olawe Island Conveyance Commission, Wailuku, Maui.
- KAUAHIKAUA, J. 1989. Geophysical investigation for ground water resources, Kaho'olawe, Hawai'i. U.S. Geol. Surv. Open-File Rep.
- LOAGUE, K. 1990. R-5 revisited: 2. Reevaluation of a quasi-physically based rainfall-runoff model with supplemental information. *Water Resour. Res.* 26: 973–987.
- . 1992a. Soil-water content at R-5: 2. Impact of antecedent conditions on rainfall-runoff simulations. *J. Hydrol.* 139: 253–261.
- . 1992b. Impact of overland flow plane characterization on event simulations with a quasi-physically based model. *Water Resour. Res.* 28: 2541–2545.
- . 1992c. Using soil texture to estimate saturated hydraulic conductivity and the impact on rainfall-runoff simulations. *Water Resour. Bull.* 28: 687–693.
- LOAGUE, K. M., and R. A. FREEZE. 1985. A comparison of rainfall-runoff techniques on small upland catchments. *Water Resour. Res.* 21: 229–240.
- MACDONALD, G. A., A. T. ABBOTT, and F. L. PETERSON. 1983. *Volcanoes in the sea: The geology of Hawaii*, 2nd ed. University of Hawai'i Press, Honolulu.
- PERROUX, K. M., and I. WHITE. 1988. Designs for disk permeameters. *Soil Sci. Soc. Am.* 52: 1205–1215.
- SKALING, W. 1992. TRASE: A product history. Pages 169–185 in G. C. Topp, W. D. Reynolds, and R. E. Green, eds. *Advances in measurement of soil physical properties: Bringing theory into practice*. Soil Sci. Soc. Am. Spec. Publ. 30.
- SOILMOISTURE. 1990. *TRASE System 1: Operating instructions*. Soilmoisture Equipment Co., Santa Barbara, California.
- SPRIGGS, M. 1987. *Preceded by forest: Changing interpretations of landscape change on Kaho'olawe*. In P. Rosendahl, A. Haun, J. Halbig, M. Kaschko, and M. S. Allen, Draft Report Kaho'olawe Excavations, 1982–3, Data Recovery Project, Island of Kaho'olawe, Hawai'i. Paul H. Rosendahl, Ph.D., Inc. Prepared for Department of the Navy, Pacific Division, Naval Facilities Engineering Command, Pearl Harbor, Hawai'i.
- STATE OF HAWAII. 1973. *Climatologic stations in Hawaii*. Rep. R-72. Department of Land and Natural Resources, Division of Water and Land Management, Honolulu.

- . 1990. Kaho'olawe water resources study: Strategies for the management of land and water resources. Rep. R-82. Watershed Management Systems. Prepared for the Protect Kaho'olawe 'Ohana/Fund, Department of Land and Natural Resources, Division of Water Resource Management, Honolulu.
- STEARNS, H. T. 1940. Geology and groundwater resources of the islands of Lanai and Kahoolawe, Hawaii. Bulletin 6, Hawai'i Division of Hydrography, Honolulu.
- . 1985. Geology of the state of Hawaii, 2nd ed. Pacific Books, Palo Alto, California.
- U.S. WEATHER BUREAU. 1962. Rainfall-frequency atlas of the Hawaiian Islands. U.S. Dep. Commer. Tech. Pap. 43.
- WHITE, I., M. J. SULLY, and K. M. PERROUX. 1992. Measurement of surface-soil hydraulic properties: Disk permeameters, tension infiltrometers, and other techniques. Pages 69–103 in G. C. Topp, W. D. Reynolds, and R. E. Green, eds. Advances in measurement of soil physical properties: Bringing theory into practice. Soil Sci. Soc. Am. Spec. Publ. 30.
- WOOLHISER, D. A. 1975. Simulation of unsteady overland flow. Pages 485–508 in K. Mahmood and Y. Yvejevich, eds. Unsteady flow in open channels. Water Resources Publications, Fort Collins, Colorado.
- ZEGELIN, S. J., I. WHITE, and G. F. RUSSELL. 1992. A critique of the time domain reflectometry technique for determining field soil-water content. Pages 187–208 in G. C. Topp, W. D. Reynolds, and R. E. Green, eds. Advances in measurement of soil physical properties: Bringing theory into practice. Soil Sci. Soc. Am. Spec. Publ. 30.